ESTIMATING SEASONAL CROP WATER CONSUMPTION IN IRRIGATED LANDS USING SOIL MOISTURE AND REFERENCE EVAPOTRANSPIRATION

by

Oliver Henry Hargreaves

A thesis submitted in partial fulfillment
of the requirements for the degree

of

MASTER OF SCIENCE

in

Civil and Environmental Engineering

Approved:

_____	_____
Alfonso Torres-Rua, Ph.D. Major Professor	L. Niel Allen, Ph.D. Committee Member
_____	_____
David Stevens, Ph.D. Committee Member	Matt Yost, Ph.D. Committee member

_____
D. Richard Cutler, Ph.D.
Interim Vice Provost of Graduate Studies

UTAH STATE UNIVERSITY
Logan, Utah

2022

ABSTRACT

Estimating seasonal crop water consumption in irrigated lands using soil moisture and reference evapotranspiration

by

Oliver Henry Hargreaves

Utah State University, 2022

Major professor: Alfonso Torres-Rua

Department: Civil and Environmental Engineering

There is significant interest from stakeholders, water agencies, and water users to adequately estimate crop water consumption, or evapotranspiration (ET), for water use monitoring and accounting purposes. ET is a key metric in irrigated agriculture, which is by far the largest user of diverted water in the American West. Therefore, accurate ET values are needed for managing the growing demand of the diminishing water resources in the West. Unfortunately, accurately determining ET is difficult and requires expensive and sophisticated instrumentation such as lysimeters, eddy covariance (EC) flux towers, or remote sensing algorithms; these approaches are cost prohibitive for most farm managers and/or require significant technical expertise and are therefore reasonable only in research settings. This study proposes the estimation of ET on a seasonal time scale using only information from soil moisture sensors along the root zone profile plus reference ET information from local weather stations for irrigated crops at four study sites in Utah. The first and second sites in Vernal and Modena respectively are dedicated to alfalfa production under sprinkler irrigation and are

equipped with an EC tower. The third and fourth sites in West Weber are dedicated to onion production under drip and furrow irrigation, respectively. Data from the Vernal study site was used to calibrate the proposed ET model, while the data from the Modena study site was used to verify whether the model would work in a different crop growing climate setting without further calibration. The West Weber sites served as a practical example of how the model can be employed to estimate seasonal ET in different irrigation settings and what insight can be gained by such estimates.

Besides testing water balance criteria to estimate ET, this study developed and tested a new empirical Soil Moisture based EvapoTranspiration (SMET) model that estimates seasonal ET based on the relationship associated with reference ET, changes in soil moisture, and actual evapotranspiration (ET_a): $if\ \Delta\theta < 0 \rightarrow \mathrm{ETa} = \alpha(\mathrm{ETr} - \Delta\theta)\ else\ ETa = 2\alpha ETr$ where α is a non-dimensional constant with a value of 0.43. The RMSE and MAE of the relationship are 1.8 mm/day and 1.1 mm/day, respectively which translates to a total seasonal difference of at most ±7% when compared to the EC tower measurements and better performance than water balance criteria. This accurate, easy-to-use, and low-cost method of estimating seasonal ET using existing soil moisture sensors along the soil profile and reference ET data could make crop water consumption information accessible to a larger number of managers, producers, and policy makers to make better-informed decisions regarding water conservation and maximizing this limited resource.

(76 pages)

PUBLIC ABSTRACT

Estimating seasonal crop water consumption in irrigated lands using soil moisture and reference evapotranspiration

by

Oliver Henry Hargreaves

Utah State University, 2022

Major professor: Alfonso Torres-Rua

Department: Civil and Environmental Engineering

The increase in population and the megadrought that the American west has been experiencing for the past two decades and for the foreseeable future are the cause of great stress on the region's water resources. In an effort to mitigate the worst effects of water shortages many public and private agencies have been pursuing ways to reduce water use while maintaining the current status quo of living standards, industrial productivity, and agricultural yield. This project aims to study water use in irrigated lands dedicated to agriculture with the objective of quantifying crop water use, often referred to as evapotranspiration (ET), as this is among the most important metrics when it comes to increasing water use efficiency, i.e., increasing the amount of agricultural output per amount of water input.

This study aims to develop a methodology that allows land managers to estimate evapotranspiration using familiar tools and data i.e., soil moisture sensors. The first study site in Vernal, Utah, was used to develop the proposed methodology because alongside the soil moisture data, accurate evapotranspiration measurements were

available which allowed for the calibration and verification of the model. The second study site in Modena, Utah, in which accurate evapotranspiration measurements were also available, was used as a testing ground for the estimates provided by the proposed methodology allowing to assess whether local calibration was required or not. The third study site in West Weber, Utah, where two irrigation methods (drip and flood irrigation) were employed, was used as a practical example of how this methodology could be implemented in a real farm scenario and what insight could be gained from it.

The proposed Soil Moisture based EvapoTranspiration (SMET) estimation model reliably provided accurate results (within ±7%) in the first two study sites where they could be compared with results from more sophisticated methods. In the third study site the SMET model offered previously hard to obtain insight on how the water use is influenced by the two irrigation techniques employed and on how water use can differ even within the same field. The encouraging results from this study prove that this user-friendly and low-cost crop water use estimation method can provide managers, producers, and policy makers with an accurate number, allowing for better-informed decisions regarding water conservation and maximizing the beneficial use of this limited resource.

This thesis is dedicated to my uncle Mark

who has been a lifelong inspiration and without whom

I would not be writing this document.

ACKNOWLEDGEMENTS

I want to express deep appreciation to my advisor Dr. Alfonso Torres for providing me the opportunity to pursue the master's degree culminating in this thesis. Alfonso has always been very enthusiastic and supportive of my work and constantly provided invaluable feedback and insight without which this project would have come to fruition. The irrigation engineering lab headed by Alfonso has been a great work environment and I am very thankful of all its current and past members, Ayman Nassar, Emre Tunca, Rui Gao, Karem Meza-Capcha, Laura Christiansen, Anderson Safre, Katherine Osorio, and Moises Duran for always being so kind, helpful, and patient.

Thank you to Dr. Lawrence Hipps, Dr. Matt Yost, Dr. Niel Allen, and Dr. Stevens for provided me with the data used for this project and with insightful recommendations on how to proceed along the way.

Thank you also to the friends I have made during my time at USU for putting up with my nonsense while providing me with countless opportunities to recreate and enjoy the natural beauties of Cache Valley and its surroundings. Thank you especially Allie for always being such an amazing life partner.

Special thanks to my family for always encouraging me to pursue my objectives and inspiring my journey through life.

CONTENTS

LIST OF TABLES

LIST OF FIGURES

1. INTRODUCTION

Water is of utmost importance for a wide range of applications from domestic, to industrial, to natural ecosystems, to agriculture and many more. Despite increases in water use by sectors other than agriculture, irrigation continues to be the main water user globally, and agriculture is responsible for 70 percent of all freshwater withdrawals worldwide (FAO 2022). This number is greater in arid regions such as Utah where historically irrigation accounts for approximately 80 percent of the freshwater use (Maughan et al. 2015) (Murray and Reeves 1977). It is a well understood fact that to maintain and increase levels of agricultural production in such arid regions, water resources need to be used in the most efficient way possible. This is especially salient in the context of human caused climate change, where temperatures are rising, and water resources are stressed due to less predictable precipitation patterns (Trenberth 2011), and the water storage is limited due to the drastic reduction is snowpack in the western United States of about 20% since 1955 (Michon Scott and Rebecca Lindsey 2022). To ensure that agricultural production keeps up with the growth rate of the global population, which is likely to reach nearly 11 billion by the end of the century (United Nations 2022), without inflicting irreversible damage to global freshwater resources, it is critical to implement cost-effective, reliable, and accessible tools to quantify current and future water availability and needs which can allow producers to make informed decisions (e.g. timing, amount) on irrigation thus increasing irrigation efficiency. Providing the tools required for land managers to obtain reliable crop water use, also known as evapotranspiration (ET), estimates can ensure water is not overallocated (e.g., overwatering crops), which not only decreases water use efficiency, but can also impede

crop development due to waterlogging (Alonso E. Rhenals and Rafael L. Bras 1981) or underirrigation, increase production costs (Keller and Bliesner 1990), and negatively impact the environment (Maughan et al. 2015). Furthermore, reasonable estimates of crop water use are necessary to employ principles of deficit irrigation, which allow for maximizing the production per unit water used (Fereres and Soriano 2007).

There is a rich literature discussing the effectiveness of using soil moisture information and ET estimates to increase water efficiency while maintaining yields but efforts to infer ET from soil moisture data are limited.

a) Dursun and Ozden 2011 showed that irrigation scheduling can be done using soil moisture sensors in a cost-effective manner.
b) Zotarelli et al. 2011 showed that soil moisture-based irrigation management can increase water use efficiency and decrease nitrogen leaching in bell peppers.
c) Migliaccio et al. 2010 showed that using soil moisture and historical ET based methods can reduce water use significantly while maintaining production levels.
d) McCready et al. 2009 showed how soil moisture sensors can reduce the irrigation amount in turfgrass without loss in quality.
e) Fereres and Soriano 2007 concluded that deficit irrigation can be used to maximize water productivity and farmers net income.
f) Scott et al. 2003 showed that high resolution thermal-infrared data collected by Landsat TM and ASTER, permit the calculation of a surface energy balance to calculate ET.

g) Akuraju et al. 2021 explored the use of thermal infrared remote sensing to estimate root zone soil moisture in agricultural fields concluding that the crop water stress index can be used with satisfactory accuracy

h) Victor Hugo de Morais Danelichen et al. 2021 aimed to evaluate the accuracy of vegetation and soil water indexes through satellite images from Landsat 5 concluding that the application of the use of remote sensing products in the management of water resources is very promising, but that they require proper use, awareness of limitations and correct interpretation of remote sensing data

i) Melton et al. 2021 showed that the remote sensing techniques used by the web based OpenET platform which uses an ensemble of six satellite-based approaches to generate field scale ET maps with an accuracy assessed by a network of EC flux tower of ±8%.

j) Kisekka et al. 2022 showed how remotely sensed evaporative fraction data can be used to estimate root zone soil moisture using machine learning approaches.

Currently, most methods used to determine ET at an agricultural field scale use crop coefficients with the Penman-Monteith ET (PM) reference equation, lysimeter measurements, eddy covariance towers measurements, or, most recently, remote sensing techniques. The PM method requires accurate data collection of weather parameters and uses crop coefficients that need to be determined or adjusted for different crops and climates (Allen, R. G. et al. 1998; Drechsler et al. 2022a). The application of lysimeters is constrained by numerous factors including the complex and expensive construction and installation processes, the complicated maintenance

operations, and their lack of automation (Ruiz-Peñalver et al. 2015). EC towers are very accurate (Gebler et al. 2015), but their cost and complexity make them inappropriate anywhere but in research settings (Markwitz and Siebicke 2019; Wei et al. 2019). Although remote sensing techniques, both satellite and drone based, will become more accessible and accurate as the technology improves it requires further refinement (Song et al. 2018) as it has limitations linked to the long data processing time and inaccuracies during certain growth stages (Diarra et al. 2017) or locations not included for validation (Melton et al. 2021).

Studies that have compared the different ET estimation methodologies include:

a) López-Urrea et al. 2006, who concluded that the FAO-56 Penman-Monteith method provided consistent ET estimates with lysimeter measurements in semi-arid regions.
b) Trajkovic and Kolakovic 2009, who compared the performance of five alternative methods to estimate ET in humid regions concluding that the Turc equation worked best.
c) Gebler et al. 2015, who showed good agreement of ET estimated using lysimeters and EC towers.
d) Song et al. 2018, who showed how ET estimates using satellite based remote sensing is possible but needs further refinement.
e) Drechsler et al. 2022b, who quantified crop water use using a soil water balance and an eddy covariance energy balance showed how accurate ET estimates can help preserve water resources in almond orchards.

It can be difficult to know what type of data farmers in a given region (e.g., Utah) collect, if any, but some of the most common and familiar data available to all land managers are soil moisture data, which can be easily and accurately be collected using a number of inexpensive options (Maughan et al. 2015), and weather data which for example is collected at over 691 sites throughout the state of Utah (Wharton 2017). Bastiaanssen et al. 2007 noted that due to the absence of the required soil, crop and weather data, and the steep learning curve of the first application of the methodology are among the reasons numerical irrigation and drainage models are underused despite the promising progress being made in the field. Building upon the water conservation efforts in agriculture that are being made in Utah (Bureau of Reclamation; Utah Division of Water Resources) this project aims to use the soil moisture data collected by farmers and land managers along with reference evapotranspiration (ETr) from a nearby weather station to provide a seasonal estimate of ET, providing a cost-effective and simple tool that can allow water users to make informed decisions when they have to decide how to use limited water resources for agricultural production. This study proposes the following research questions:

1) Is it possible to obtain an accurate estimate of seasonal crop ET by using only familiar or available information such as soil moisture measurements and ETr? To answer this question a model that uses only SM and ETr as inputs was developed and tested against EC tower measurements.
2) What insights can seasonal ET estimates made by the proposed model provide on different irrigation practices? To answer this question the model was implemented in

two nearby fields that used different irrigation techniques and the results were compared to each other.

2. MATERIALS AND METHODS

2.1. Study sites

The study sites for this project were four agricultural fields in Utah, one in Vernal, one in Modena and two in West Weber (*Figure 1, Table 1*). Utah is mostly classified as a semi-arid region with hot, dry summers and cold winters with most of the annual precipitation occurring during the winter months (Gillies and Ramsey 2009). Utah's mean altitude is 1835 m, mean precipitation is 359 mm, mean temperature is 9.2 $^{\circ}$C, and mean solar radiation is 17 MJ/m^{2}day (PRISM Climate Group at Oregon State University). The specific climate parameters for each study site are reported in *Table 1*.

The Vernal and Modena study sites are equipped with an EC flux tower, a weather station, and an array of soil moisture sensors; both sites are dedicated to perennial alfalfa production under sprinkler irrigation. While the SM sensors of the Vernal study site are in close proximity to the EC tower, there are two sets of SM sensors in the Modena study site: north and east (*Figure 1*). The two West Weber study sites are equipped with soil moisture sensors at three locations in each field; both fields are dedicated to onion production in cultivated beds, but while the first employs flood irrigation (West Weber 1), the second uses drip irrigation (West Weber 2).

Figure 1: Maps of the four study sites discussed in this paper. Vernal and Modena are alfalfa fields with sprinkler irrigation and West Weber 1 and 2 are onion field with flood and drip irrigation respectively.

Table 1: Study site details. Elevation, precipitation, mean temperature, and solar radiation values are the 30-year normals retrieved from the PRISM climate group at Oregon State University.

Study site	***Vernal***	***Modena***	***West Weber 1***	***West Weber 2***
Longitude (DD)	-109.564270	-113.789074	-112.084059	-112.084065
Latitude (DD)	40.457876	37.747303	41.240400	41.240494
Crop	Alfalfa	Alfalfa	Onion	Onion
Irrigation	Sprinkler	Sprinkler	Flood	Drip
Area (Ha)	31.7	51.1	6.2	7.1
Growing season	2019-2020	2021	2019	2019
Elevation (m)	1703	1596	1291	1291
Precipitation (mm)	261	286	416	416
Mean Temperature (°C)	8.1	9.5	11.1	11.1
Mean Solar Radiation (MJ/m^2day)	17.2	18.5	16.4	16.4
EC flux tower	Yes	Yes	No	No
SM measuring locations	1	2	3	3

2.2. Methodology

The overall methodology followed for the analysis performed at each site is presented in the flowcharts in *Figure 2* and discussed in detail in the following sections.

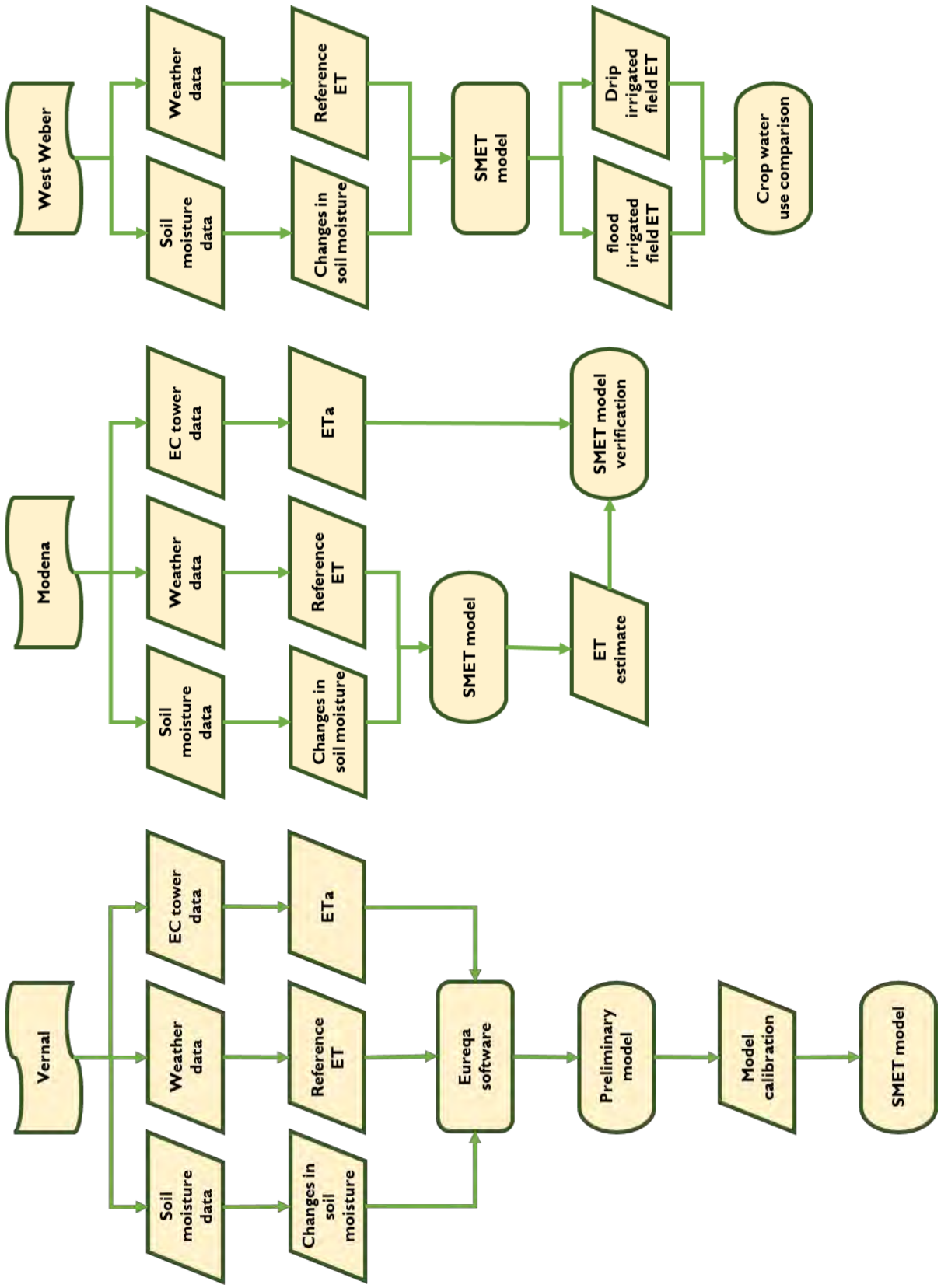

Figure 2: Flowcharts of the methodologies followed for the analysis performed at the three study sites described in this study.

2.3. Soil moisture data

2.3.1. Soil moisture data collection

The volumetric water content data at each site was collected using a site-specific array of time reflectance domain (TDR) sensors (*Figure 3*) (Acclima), according to the manufacturer's specifications the reporting accuracy of the sensors is ±1% for coarse and medium textured soils and ±2.5% for fine textured soils (Acclima 2022). Details of the installation depths at each site are presented below (*Figure 4*).

Figure 3: The Acclima TDR 315 sensor used to collect soil moisture data.

Vernal

The raw soil moisture (SM) data was collected in proximity of the EC flux tower (*Figure 1*) by 7 TRD sensors (*Figure 3*) every 15 minutes. The 7 sensors were spaced out vertically at increasing depths (*Figure 4*): 3, 10, 25, 65, 105, 145, and 215 cm (1, 4, 10, 26, 41, 57, and 85 in). The sensor depths for the Vernal site were selected to represent the different horizons that are part of the root zone which for alfalfa can reach up to ~2 m (~80 in).

Modena

The raw soil moisture data was collected in two locations in the field, East and North (*Figure 1*) at midnight. The East location had an array of 7 TRD soil moisture sensors (*Figure 3*) installed at increasing depths (*Figure 4*): 8, 15, 30, 61, 91, 122, and 152

cm (3, 6, 12, 24, 36, 48, and 60 in). The North location had an array of 6 TRD soil moisture sensors (*Figure 3*) installed at increasing depths (*Figure 4*): 8, 15, 30, 61, 91, and 122 cm (3, 6, 12, 24, 36, and 48 in); the 152 cm deep sensor was not installed in the North field due to the presence of a hard-to-penetrate gravel layer that was not part of the root zone. The sensor depths at the Modena site did not follow represent the natural soil horizons, rather they were installed by keeping in mind that most of the plant roots are concentrated in the topsoil layers which is where that the greatest changes in soil moisture occur. This rationale led to having a close spacing near the surface to best monitor soil moisture in the topsoil layers and a greater spacing at deeper depths to monitor soil moisture for the remainder of the rooting depth, which is expected to vary to a lesser extent.

West Weber

The raw soil moisture data was collected by 10 TRD soil moisture sensors (*Figure 7*) every 30 minutes at three sites in each of the two fields, stations 101, 102, and 103 for in the flood irrigated field and stations 104, 105, and 106 in the drip irrigated field (*Figure1*). There are six sensors under the onion bed (sensors 1, 2, 4, 5, 7, and 8) which is 58 cm (23 in) wide, three sensors under the furrow (sensors 3,6,9) which is 41cm (16 in) wide, and one sensor that is common to both the onion bed and the furrow (sensor 10); sensors 1, 2, and 3 are 10 cm (4 in) deep; sensors 4, 5, and 6 are 25 cm (10 in) deep; sensors 7, 8, and 9 are 56 cm (22 in) deep; sensor 10 is 91 cm (36 in) deep (*Figure 4*). The sensor depth were chosen to represent the onion root zone which typically extends no deeper than ~60 cm (~24 in).

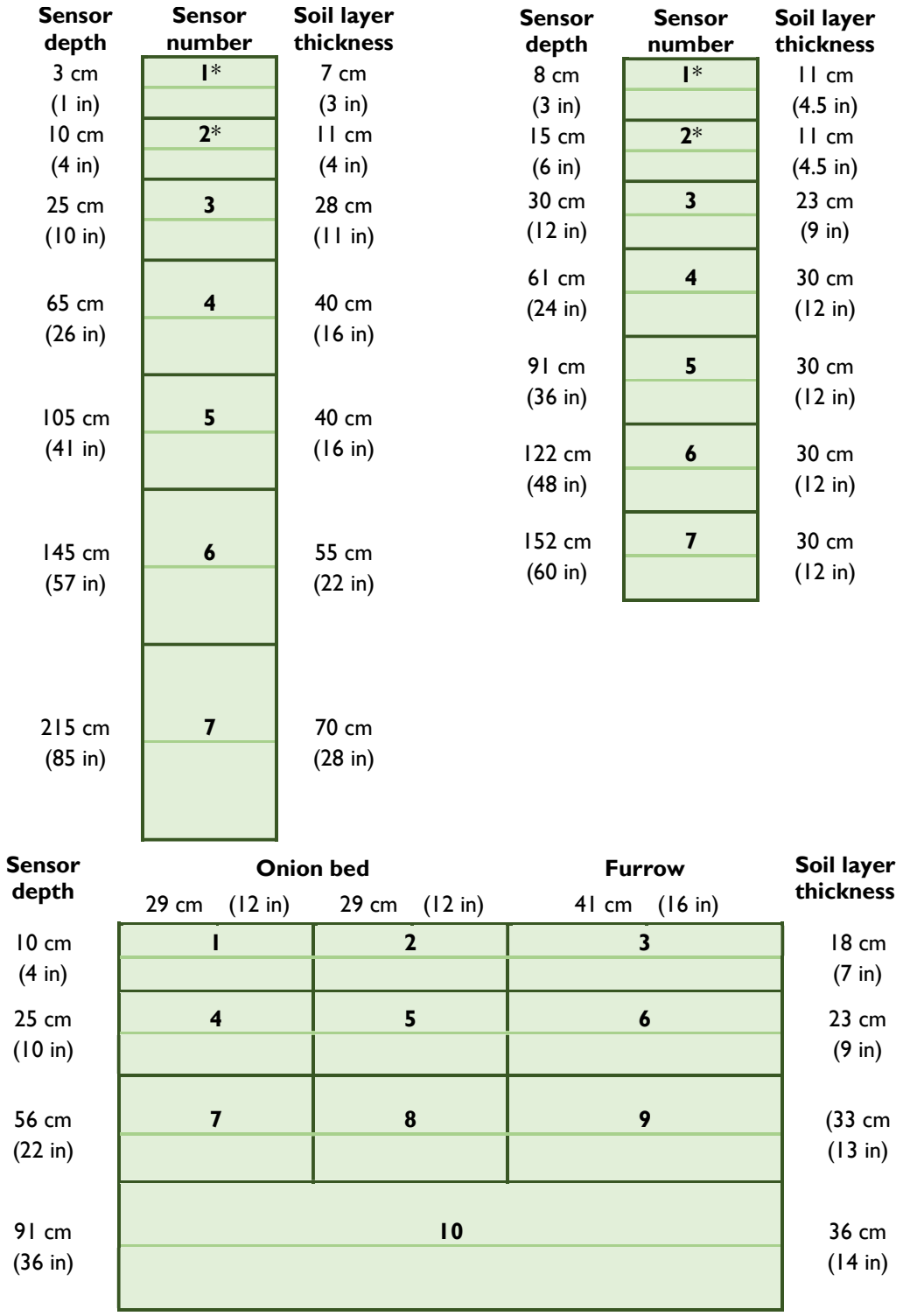

*Figure 4: Soil moisture sensor arrays for the Vernal (top left), Modena (top right), and the West Weber (bottom) study sites. * Soil layers 1 and 2 are not to scale for the Vernal and Modena sites.*

2.3.2. Soil moisture timeseries

Vernal

By observing the soil moisture data for the Vernal study site (*Figure 5*) several irrigation events can be made out as they coincide with rapid increases followed by gradual decreases in volumetric water content. The irrigation caused spikes can be more easily

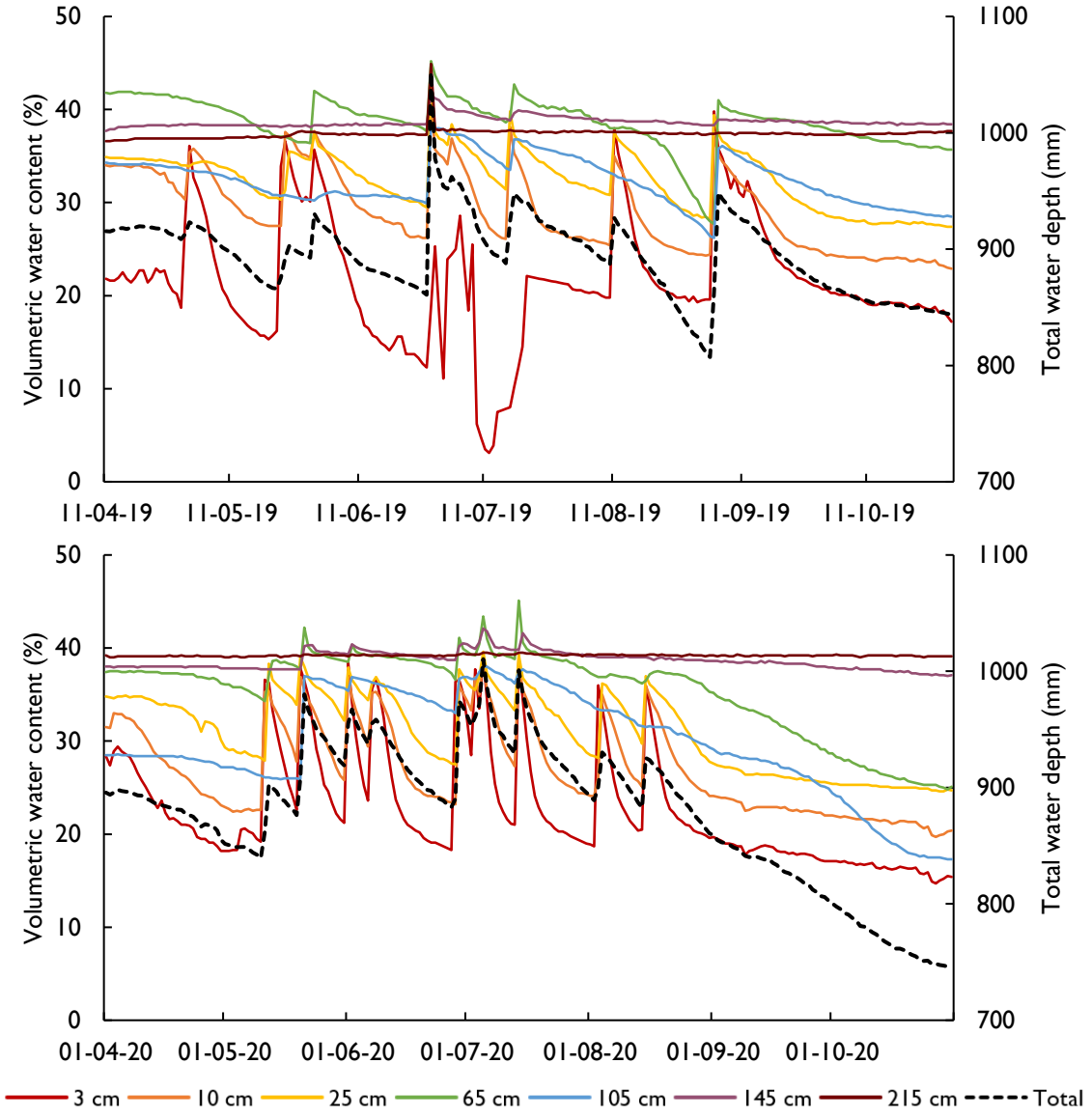

Figure 5: Midnight soil moisture data for the 2019 and 2020 growing seasons in Vernal. The Left axis indicates the volumetric water content at the various soil sensor depth. The Right axis indicates the total soil water depth in the soil profile in mm.

observed in the shallower soil moisture timeseries (3, 10, and 25 cm deep) and becomes more subtle with the increase of depth until they become almost impossible to discern in the deepest layer (215 cm deep). For additional soil moisture information, see the soil moisture profiles (volumetric water content ~ depth) for the Vernal site in Appendix B.

Modena

The soil moisture timeseries from the two stations in the Modena study sites (*Figure 6*) reveal how the irrigation scheduling was more frequent than for the Vernal study site, on the order of days rather than weeks. Note that while the deepest soil moisture sensor from the East location is at 152 cm (60 in) the deepest sensor at the North location is at 122 cm (48 in); this is due to the presence of a gravel layer in the North field that made it impractical to install the deeper sensor. For additional soil moisture information, see the soil moisture profiles (volumetric water content ~ depth) for the Modena site in Appendix B.

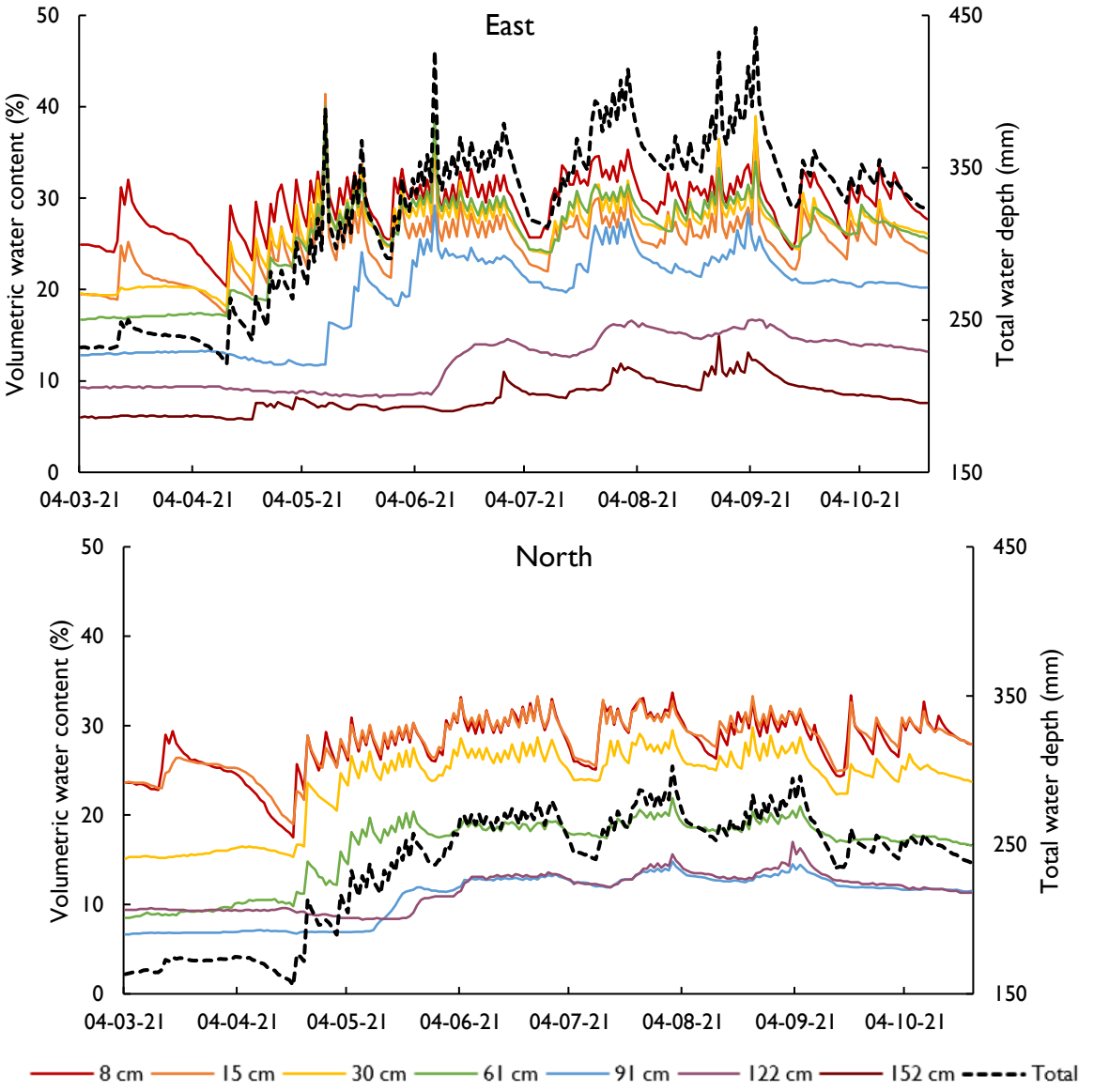

Figure 6: Soil moisture timeseries for the East (top) and North (bottom) stations in the Modena study site for the 2021 growing season. The Left axis indicates the volumetric water content at the various soil sensor depth. The Right axis indicates the total soil water depth in the soil profile in mm.

West Weber

The soil moisture sensor array of the West Weber study sites allows to appreciate the difference in water application between a flood irrigated and a drip irrigated field when looking at the soil moisture timeseries (*Figures 7 and 8*). The most dramatic difference is observed in the furrow which in the flood irrigated field (stations 101, 102, and 103) consistently has a total water depth ~400 mm while it has a depth of only ~250 mm in the drip irrigated field (stations 104, 105, and 106). This should come to no surprise since the flood irrigated field regularly floods the furrow to saturate the soil with the drip irrigated field having a drip line along the onion bed ensuring that the water largely stays within the root zone as demonstrated by the deepest set of sensors (91 cm deep) being always near saturation at ~40% in the flood irrigated field and much lower at ~10-30% in the drip irrigated field.

The soil moisture timeseries of the drip irrigated field also offer insight on a common problem incurred by drip irrigation systems where, as the distance to the water source increases, station 104 being the nearest and 106 being the furthest, there is a loss of pressure that causes less water to be applied at the far end of the field. Because of this the total amount of water at station 104 (~300mm) is consistently higher than at the stations 105 and especially 106 (~250 mm and ~ 200 mm respectively). When this occurs caution must be exercised to avoid yield loss due to water stress.

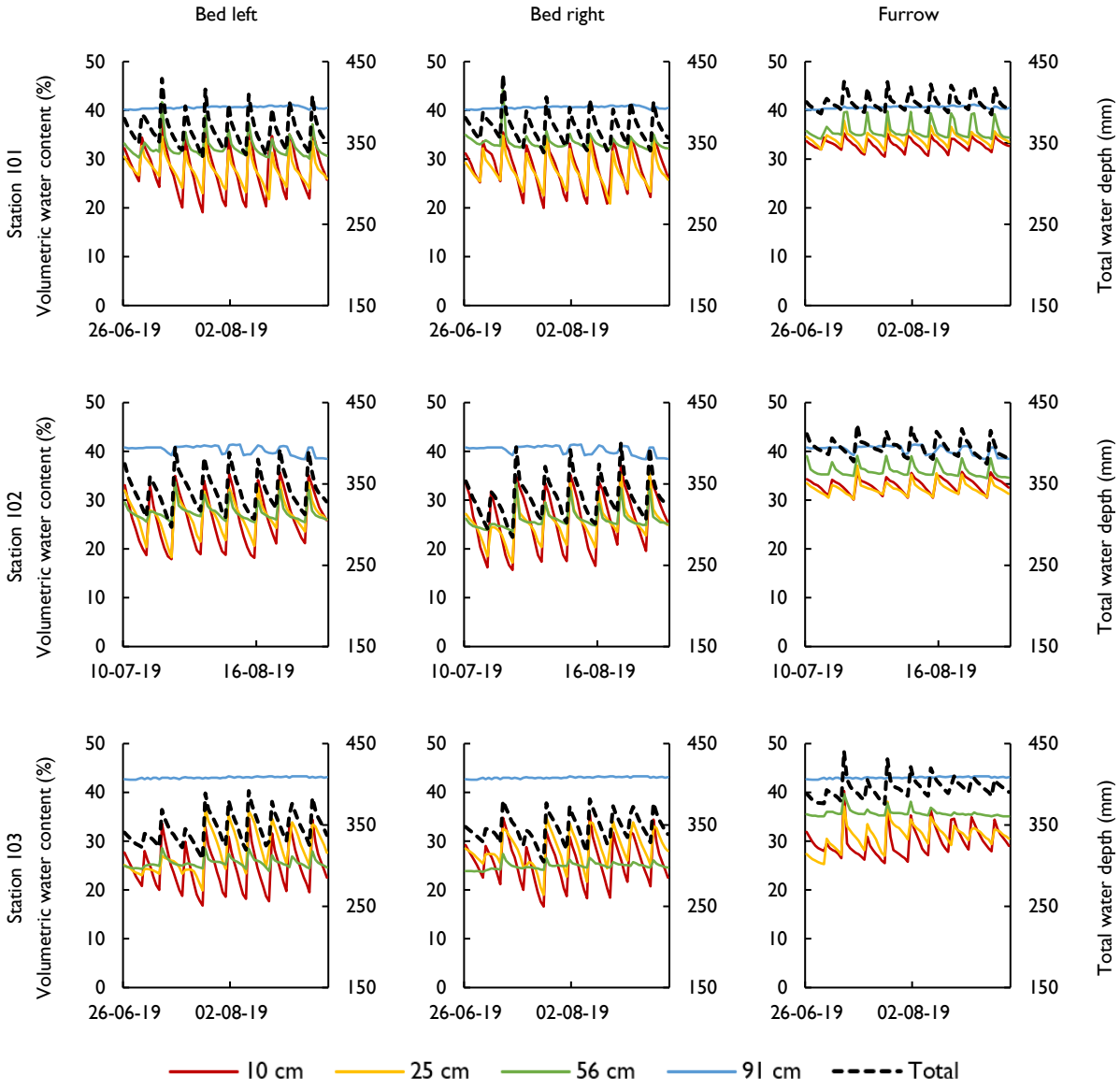

Figure 7: Soil moisture data for the flood irrigated field in West Weber for the 2019 growing season. The left axis indicated the volumetric water content at the various sensor depths. The right axis indicates the total soil water depth in the profile in mm. Note that at each station the bed and the furrow share the deepest sensor (91 cm).

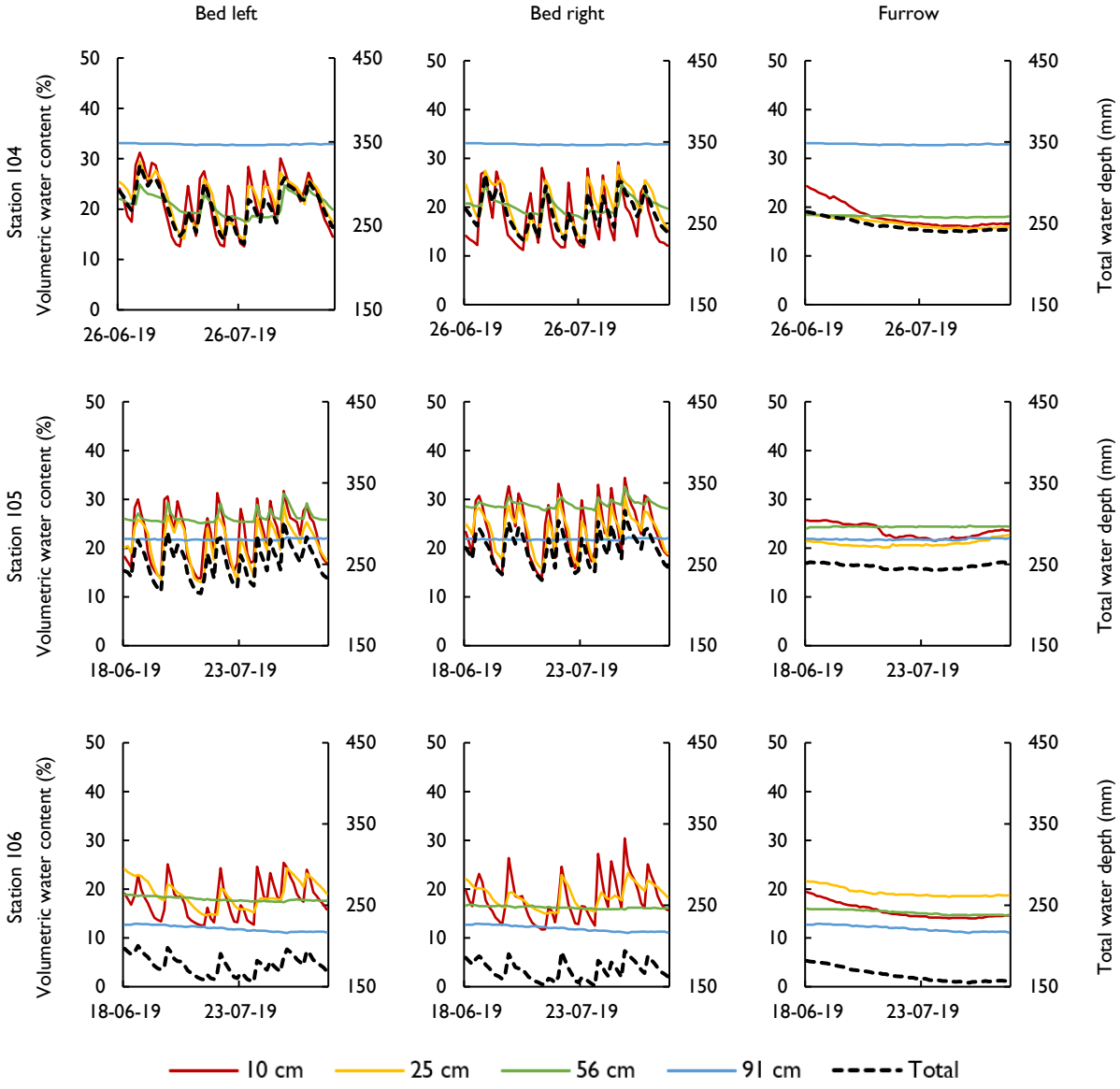

Figure 8: Soil moisture data for the drip irrigated field in West Weber for the 2019 growing season. The left axis indicated the volumetric water content at the various sensor depths. The right axis indicates the total soil water depth in the profile in mm. Note that at each station the bed and the furrow share the deepest sensor (91 cm).

2.3.3. Data quality assurance and quality control

The quality assurance and quality control (QAQC) for the soil moisture sensors checked primarily for two things:

a) Reasonable measurements of volumetric water content (VWC): values greater than 60% were discarded. This threshold was selected by observing that VWC after intense irrigation events does not exceed the 40-50%, therefore values greater than 60% were assumed to be a misreading which are typically due to rocky soils or pockets of air around the sensors which fill with water.
b) Continuity in the data: missing values were estimated using linear interpolation. This only occurred in very few instances and the trend of the values was verified to be monotonic.

2.3.4. Soil moisture data preparation

Midnight data extraction

Since the methodology proposed in this paper requires only one SM measurement a day the midnight values were used. This was determined to be preferable to using the daily average value because it makes the peaks and valleys more pronounced, which makes it easier to pick up on changes in SM. Additionally, this makes sense from an "accounting" point of view: to determine how the soil moisture changed over the course of a given day one can simply calculate the difference from two successive midnight values, when plant transpiration processes are minimal (Caird et al. 2007).

Conversion from volumetric water content to water depth

The volumetric water content (given in percentage) was multiplied by the soil depth corresponding to each reading to determine the total water depth for the entire soil profile. Since the sensor array differed from site to site the calculations to convert VWC into total water depth were site specific, but the applied principle of multiplying the VWC by the soil depth corresponding to each reading was identical: $D = \sum \theta z$.

Vernal

Soil layers were assigned to each sensor by dividing the distance between each one halfway giving the following soil layer representation (*Figure 4*):

1) Sensor 1: $z_1 = [0,\ 0.07]\ \mathrm{m} = 7\ \mathrm{cm}$
2) Sensor 2: $z_2 = [0.07,\ 0.18]\ \mathrm{m} = 11\ \mathrm{cm}$
3) Sensor 3: $z_3 = [0.18, 0.45]\ \mathrm{m} = 28\ \mathrm{cm}$
4) Sensor 4: $z_4 = [0.45,\ 0.85]\ \mathrm{m} = 40\ \mathrm{cm}$
5) Sensor 5: $z_5 = [0.85,\ 1.25]\ \mathrm{m} = 40\ \mathrm{cm}$
6) Sensor 6: $z_6 = [1.25,\ 1.80]\ \mathrm{m} = 55\ \mathrm{cm}$
7) Sensor 7: $z_7 = [1.80,\ 2.50]\ \mathrm{m} = 70\ \mathrm{cm}$

With this the total soil profile water content can be calculated as the sum of each sensor reading multiplied by the soil depth represented by each sensor:

Equation 1

$$\mathrm{D} = \sum_{i=1}^{7} \theta_i d_i =$$

$$= \theta_1 z_1 + \theta_2 z_2 + \theta_3 z_3 + \theta_4 z_4 + \theta_5 z_5 + \theta_6 z_6 + \theta_7 z_7$$

Modena

Just like with the Vernal site the soil layers were assigned to each sensor by dividing the distance between each one halfway giving the following soil layer representation (*Figure 4*):

1) Sensor 1: $z_1 = [0,\ 0.11]\ \mathrm{m}\ = 11\ \mathrm{cm}$
2) Sensor 2: $z_2 = [0.11,\ 0.23]\ m = 11\ cm$
3) Sensor 3: $z_3 = [0.23, 0.46]\ m = 23\ cm$
4) Sensor 4: $z_4 = [0.46,\ 0.76]\ m = 30\ cm$
5) Sensor 5: $z_5 = [0.76,\ 1.07]\ m = 30\ cm$
6) Sensor 6: $z_6 = [1.07,\ 1.37]\ m = 30\ cm$
7) Sensor 7: $z_7 = [1.37,\ 1.68]\ m = 30\ cm$

With this the total soil profile water content can be calculated as the sum of each sensor multiplied by the soil depth represented by each sensor with *Equation 2*.

West Weber

The total water depth for the West Weber study sites in a similar manner as for the Vernal study site with the key difference being that two values were calculated for the onion bed ($\mathrm{D_{B1}}$ and $\mathrm{D_{B1}}$) and one value was calculated for the furrow ($\mathrm{D_F}$) (*Figure 4*).

1) Sensor 1, 2, 3: $\mathrm{z_1 = z_2 = z_3 = [0,\ 0.18]\ m\ = 18\ cm}$
2) Sensor 4, 5, 6: $z_4 = \mathrm{z_5 = z_6} = [0.18,\ 0.41]\ m = 23\ cm$
3) Sensor 7, 8, 9: $z_7 = \mathrm{z_8 = z_9} = [0.41, 0.74]\ m = 33\ cm$
4) Sensor 10: $z_{10} = [0.74,\ 0.109]\ m = 36\ cm$

Equation 2 $\quad \mathrm{D}_{B1} = \sum_i^{1,4,7,10} \theta_i z_i = \mathrm{\theta_1 z_1 + \theta_4 z_4 + \theta_7 z_7 + \theta_{10} z_{10}}$

$$D_{B2} = \sum_i^{2,5,8,10} \theta_i z_i = \theta_2 z_2 + \theta_5 z_5 + \theta_8 z_8 + \theta_{10} z_{10}$$

$$D_F = \sum_i^{3,6,9,10} \theta_i z_i = \theta_3 z_3 + \theta_6 z_6 + \theta_9 z_9 + \theta_{10} z_{10}$$

The values for the bed and for the furrow were kept separate to allow the calculation and comparison of the ET values as discussed in section 3.3 later in this paper.

2.4. Meteorological data

The only datum other than soil moisture used in this study is reference ET (ETr), which is often provided as part of readily available weather data from state weather networks. If ETr data is not readily available it can easily be calculated using the freely available RefET software (Kimberly Research and Extension Center) from the following measurements: solar radiation, precipitation, average wind speed, average atmospheric vapor pressure, mean air temperature, latitude, longitude, and elevation (Allen 1999). If only minimal weather data is available, the 1985 Hargreaves equation can be used to calculate ETo using only minimum and maximum air temperature (Hargreaves et al. 1985, 2003).

The ETr data for the Vernal and Modena study sites was collected by weather stations maintained by the Utah Climate Center and was downloaded from their website (Utah State University) in which the stations names are *Vernal* and *Modena* respectively. The ETr data for the West Weber project sites was calculated from in situ weather measurements using the RefET software using the standardized form of the ASCE Penman-Monteith method.

2.5. Eddy covariance flux tower data

As previously mentioned, the Vernal and Modena study sites have had an eddy covariance flux tower installed in the field since the fall of 2017 and spring 2021 respectively. Although EC flux tower measurements are often used to validate ET models (Franssen et al. 2010; Markwitz and Siebicke 2019; Kisekka et al. 2022; Drechsler et al. 2022a), they do not provide a single value but rather a range within which the ETa is expected to be due to the closure of the energy balance (Foken and Foken1 2008; Franssen et al. 2010). This is due to the sensors measuring ET both from the atmospheric fluxes, $ET_{original}$, and from energy fluxes, ET_{closed} (*Figure 9*). When it was impractical to use a range, the geometric mean of the original and closed ET measurements was calculated and considered to be the best approximation possible of ETa.

Equation 3 $$ETa = \sqrt{ET_{original} \cdot ET_{closed}}$$

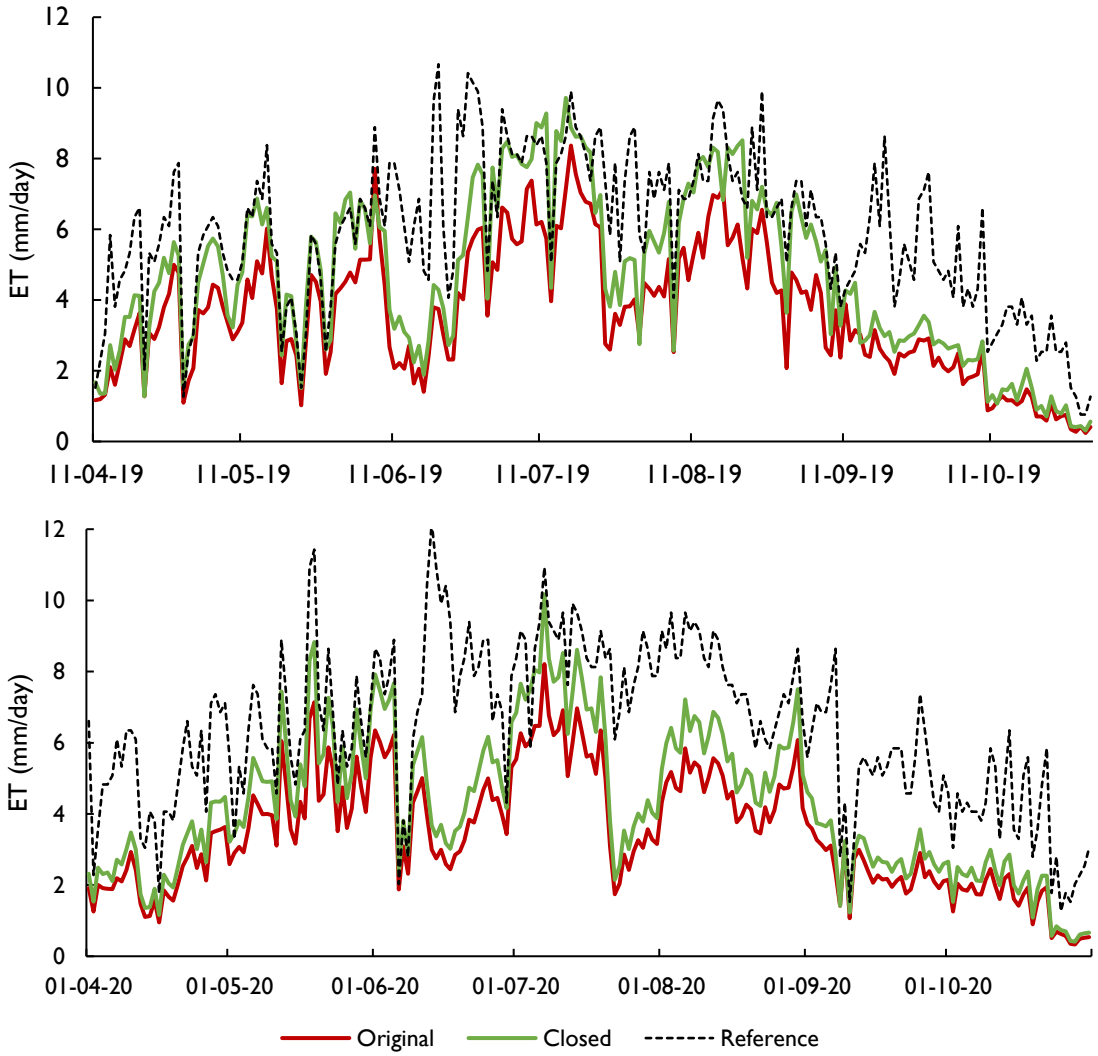

Figure 9: EC flux tower data for the Vernal study site in 2019 and 2020. The original and closed ET values represent the measurement before and after forcing the closure on the energy balance respectively. Reference ET is measured by the Vernal weather station and retrieved from the USU Utah climate center website.

2.6. Model description

The ET estimation model proposed in this paper builds upon two well understood principles that are often used to quantify crop water use: (1) the water balance method and (2) the crop coefficient method. The water balance method is a mass balance (the change in storage is equal to the sum of all inputs minus the sum of all

outputs) that used observations of the water budget components, i.e., precipitation (P), runoff (RO), and water storage change (Δθ), to compute ET as the residual (Wan et al. 2015):

Equation 4 $\Delta\theta = I + P - ET - RO + G - DP$

Where Δθ is the change is soil water storage in the root zone in mm, P is precipitation, I is irrigation, ET is evapotranspiration, RO is runoff, G is groundwater contribution, and DP is deep percolation (*Figure 6*). Although a simple model in theory, the water balance is very hard to apply in practice due to the difficulty in accurately measuring the individual terms; this is especially true for deep percolation (Walker and Skogerboe 1987) and ground water contributions and, to a lesser extent, irrigation, and runoff. These difficulties make it so that when the water balance method is implemented on a farm scale outside of research setting the results cannot be considered reliable. Nevertheless, a simplified version of the water balance can be implemented by using the following assumptions:

a) On days with absence of irrigation and precipitation: $I = P = 0$

b) Well drained soils i.e., soil moisture is at or below field capacity: $RO = DP = 0$

c) Water table well below the root zone: $G = 0$

When these three assumptions are contemporarily true, during non-irrigation/precipitation days and after gravitational water is removed from the profile, *Equation 4* can be rewritten as:

Equation 5 $ETa = -\Delta\theta$

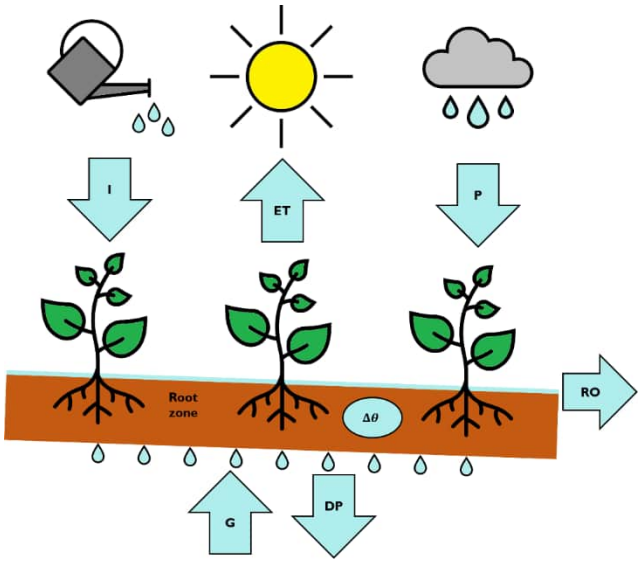

Figure 10: Water balance model scheme. The components of the water balance that drive changes in soil moisture (△θ) are represented by the arrows, when the arrow is pointing toward the plants drive an increase in soil moisture, while the arrows that point away drive a decrease in soil moisture.

Since Equation 5 is not unique and will be affected by soil characteristics (i.e., water retention) as well as water movement following irrigation events when RO, G, and DP are still present all that can be said without further verification is that:

$$ETa = f(-\Delta\theta) \quad \text{Equation 6}$$

The crop coefficient method utilizes a reference value for ET that represents the atmospheric demand (i.e., either ETr or ETo) and multiplies it by a value, the crop coefficient (Kc), that is specific to the crop and the growth stage to estimate ETa (Allen, R. G. et al. 1998):

$$ETa = Kc \cdot ETr \quad \text{Equation 7}$$

In regions such as Utah, with distinct summer and winter periods, the crop growing season closely follows the pattern of positive atmospheric water demand after the snow season, meaning that crops in the development or maturity stages will have

similar water use as reference crops (e.g., alfalfa), therefore the following relationship can be written:

Equation 8 $$ETa = f(ETr)$$

Equations 6 and 8 show how ET is a complex phenomenon that can be modeled as the part of the water cycle, but also as biophysical process that responds to environmental factors. Solving for ET within the complete water balance requires the use of advanced modeling software such as HYDRUS 1-D which uses linear finite elements to numerically solve the Richards equation for saturated–unsaturated water flow and Fickian-based advection–dispersion equations for both heat and solute transport (Šimůnek et al. 2008). The use of this type of complex software requires training and is not feasible for most land managers outside of research settings. The method proposed in this paper attempts to combine and greatly simplify *Equations 6 and 8* by expressing ET as a function of only the changes in the soil water depletion ($\Delta\theta$) and the atmospheric demand (ETr), which can both be measured with ease:

Equation 9 $$ETa = f(\Delta\theta, ETr)$$

ETa being the actual value of daily ET, since the ET measurements performed using the EC flux tower are the best available estimate, in this paper will be considered actual ET. ETr is the daily reference ET, calculated as described in section 2.3. $\Delta\theta$ is the change in soil water content of the entire profile, calculated as described in section 2.3.3, between two successive midnight values.

2.6.1. ETa approximation for irrigation days

Equation 9 is designed to work only for days when $\Delta\theta$ is negative i.e., days when the soil moisture of the soil profile as a whole is decreasing (depletion), this means that during days when irrigation (or precipitation) is occurring thus not fulfilling the assumptions for *Equation 5*. During the days when soil moisture is increasing ($\Delta\theta > 0$) due to either irrigation or rainfall, there is expected to be plenty of plant available water (PAW) which means that ET is likely to be energy limited rather than water limited; under these circumstances ETa is expected to be more strongly correlated with ETr than with soil moisture conditions. A similar approximation for irrigation days is presented in chapter 7 of FAO 56 (Allen, R. G. et al. 1998).

Equation 10 $$if\ \Delta\theta > 0 \rightarrow\ ETa \approx ETr$$

2.6.2. Outlier detection and correction

In some instances, due to excessive irrigation, rapid drainage, and/or rocky layers the soil moisture depletion data presented a large variation that do not fit the assumptions for *Equation 6*. To automate the process of outlier detection and correction, a filter capable of detecting ET estimates derived from *Equation 9* above a certain threshold and replacing them with a maximum value was designed. The filter calculates the ratio of estimated ET over ETr and compares them to a maximum crop coefficient (Kc_{max}) that is reasonable for a specific crop; if the ratio is greater than Kc_{max} then the daily ET value is set to be equal to the ETr times Kc_{max}:

Equation 11 $$if\ \frac{ET}{ETr} > \mathrm{Kc}_{max} \rightarrow ETa \approx \mathrm{Kc}_{max} \cdot ETr$$

Note that Kc_{max} can be determined from literature (e.g., FAO 24, FAO 56).

2.6.3. ETa modeling using soil moisture and ETr

Equations 9, 10, and 11 tell us that ETa is a function of ETr and Δθ when Δθ<0 and a function of only ETr when Δθ>0, nevertheless the relationship between ETa, ETr and Δθ is unknown; to determine this relationship the information available to this project was fed into the genetic programming software, with the objective of finding an equation capable of solving for ETa using only ETr and Δθ as inputs. The software used was Eureqa version 1.24.0 (note that this software is no longer publicly available, but the authors can provide a private copy), which uses symbolic regression for detecting equations and hidden mathematical relationships in raw data (Schmidt and Lipson 2009; Dubčáková 2011). Eureqa has already been proven to be useful in the hydrology field in studies aiming at improving of the Hargreaves-Samani equation in arid China (Xu et al. 2016), and the estimation of soil moisture (Aboutalebi et al. 2019).

2.7. Analysis

The data analysis of this project consisted of three phases: (1) model calibration using the data from the Vernal study site, (2) testing the model using the Modena study site without further calibration, and (3) an example of a practical application of the model at the West Weber study sites that compared estimated ET under different irrigation technologies (drip vs flood irrigation).

2.7.1. Vernal study site

The presence of an eddy covariance flux tower providing reliable measurements of ETa (as described in section 2.4), in conjunction with a deep reaching array of high-quality soil moisture sensors made the Vernal study site an ideal candidate for the verification and calibration of the proposed model.

Once the total SM was calculated as described in section 2.2.3, $\Delta\theta$ was determined as the difference between the total SM value of a certain day minus the value of the previous day. The daily estimate of ET was then calculated using the model provided by the Eureqa software from April 4th to October 31st, 2019, and from April 11th to October 31st, 2020. The obtained daily ET estimates were then used in conjunction with the daily ET measurements from the EC tower (ETa) to calculate the residuals, the root mean square error (RMSE), and the mean absolute error (MAE):

$$\sigma = ETa - ET_{Estimate}$$

$$RMSE = \sqrt{\frac{\sum_{i=1}^{n} \sigma^2}{n}}$$

$$MAE = \frac{\sum_{i=1}^{n} |\sigma_i|}{n}$$

The fitting of the model was then performed by setting the mean of the residuals equal to zero ($\overline{\sigma} = 0$) using the Solver function in MS Excel (Microsoft).

2.7.2. Modena study site

The model proposed by Eureqa and optimized with the Vernal study site data was used to estimate seasonal ET at the two soil moisture monitoring locations in the

Modena field (*Figure 1*); these estimates were then averaged to obtain a field average value which was compared against the EC tower measurements. This comparison allowed us to test whether the model would provide reasonable estimates of seasonal ET in a site with different climate, soil, and irrigation scheduling, without the need for further calibration.

2.7.3. West Weber study sites

The total soil moisture values from the three locations in each field, calculated as described in section 2.3.3, were used to calculate the daily ET estimate using the model proposed by Eureqa and optimized using the Vernal study site data, without any further calibration. These daily estimates were then used to calculate cumulative values (18 samples total: two fields, three locations, and three samples each) which in turn were used to get an average of the ET for both the onion bed and the furrow at the three locations in each field; the values from the three locations were then averaged to obtain a value for the cumulative ET from the bed and furrow for each field.

$$ET_{Flood,\ Bed} = \frac{\sum\left(ET_{101,B1}, ET_{101,B2}, ET_{102,B1}, ET_{102,B1}, ET_{103,B1}, ET_{103,B2}\right)}{6}$$

$$ET_{Flood,\ Furrow} = \frac{\sum\left(ET_{101,F},\ ET_{102,F},\ ET_{103,F}\right)}{3}$$

$$ET_{Drip,\ Bed} = \frac{\sum\left(ET_{104,B1}, ET_{104,B2}, ET_{105,B1}, ET_{105,B1}, ET_{106,B1}, ET_{106,B2}\right)}{6}$$

$$ET_{Drip,\ Furrow} = \frac{\sum\left(ET_{104,F},\ ET_{105,F},\ ET_{106,F}\right)}{3}$$

The field estimate can then be obtained with a weighted average using the width of the bed and furrow.

$$ET_{Flood} = \frac{2 \cdot 29\ cm \cdot ET_{Flood,Bed} + 41\ cm \cdot ET_{Flood,Furrow}}{2 \cdot 29\ cm + 41\ cm}$$

$$ET_{Drip} = \frac{2 \cdot 29\ cm \cdot ET_{Drip,Bed} + 41\ cm \cdot ET_{Drip,Furrow}}{2 \cdot 29\ cm + 41\ cm}$$

These cumulative values were then compared to obtain an absolute and a relative difference in seasonal ET to assess the differences in seasonal crop water consumption due to the two irrigation technologies.

3. RESULTS AND DISCUSSION

3.1. Data exploration – Water balance approach

During the data exploration phase of this project several prior attempts were made to solve the water balance, but no satisfactory solution ($RMSE < 1.5\ mm/day$) was found. As discussed in section 2.6, theoretically ETa can be calculated as the residual of *Equation 4* when all other terms are known or can be estimated. The first attempt to solve the water balance for ET was made by assuming that during non-irrigation days the only non-zero terms in *Equation 4* were the change in soil moisture ($\Delta\theta$) and ET and during irrigation days ET is equal to the reference value (i.e., ETr); this would allow to estimate daily ET simply by comparing the total soil moisture at midnight of successive days as shown in *Equation 5*. During irrigation days, and the following 2 days, soil moisture recharge and water movement in the soil profile were significant causing gaps in the daily ETa estimates; when this occurred the ETa estimates were obtained by applying *Equation 7* with interpolated Kc values.

Results from this method for the Vernal site during the 2019 and the 2020 growing seasons along with the EC tower measurements are shown in *Figure 11*;

although the estimates generally follow a similar trend to the EC tower measurements over the growing season, the method is often over- or underestimating ETa in both years. The model accuracy was quantified by comparing the daily estimates to ETa (*Equation 3*) and calculating the Pearson correlation coefficient (r), the root mean square error (RMSE) and the relative root square error (RRSE) (*Table 2*). The second metric used to evaluate model performance is verifying whether the cumulative estimate falls within the EC tower measurement range $\left(ET_a \in \left[ET_{original}, ET_{closed}\right]\right)$ on a monthly and seasonal (*Figures 12 and 13*) timescale. In 2019 only the September estimate falls within the EC tower range and is underestimating during all the other months and during the growing season. In 2020 the estimate is accurate in May, June, July, and for the entire season and is either over or underestimating the rest of the time. A possible reason for the water balance underestimation can be attributed to (1) the surface water that accumulates after irrigation and precipitation and evaporates before penetrating the soil and to (2) dew which can be a significant factor in the water balance in semi-arid regions such as Utah (Malek et al. 1999).

Table 2: Summary statistics of the water balance model estimate compared to the EC tower measured value. Higher r and smaller RMSE and RRSE values indicate better performance.

	2019	**2020**
r	0.61	0.72
RMSE	2.15 mm	1.66 mm
RRSE	1.05 mm	0.90 mm

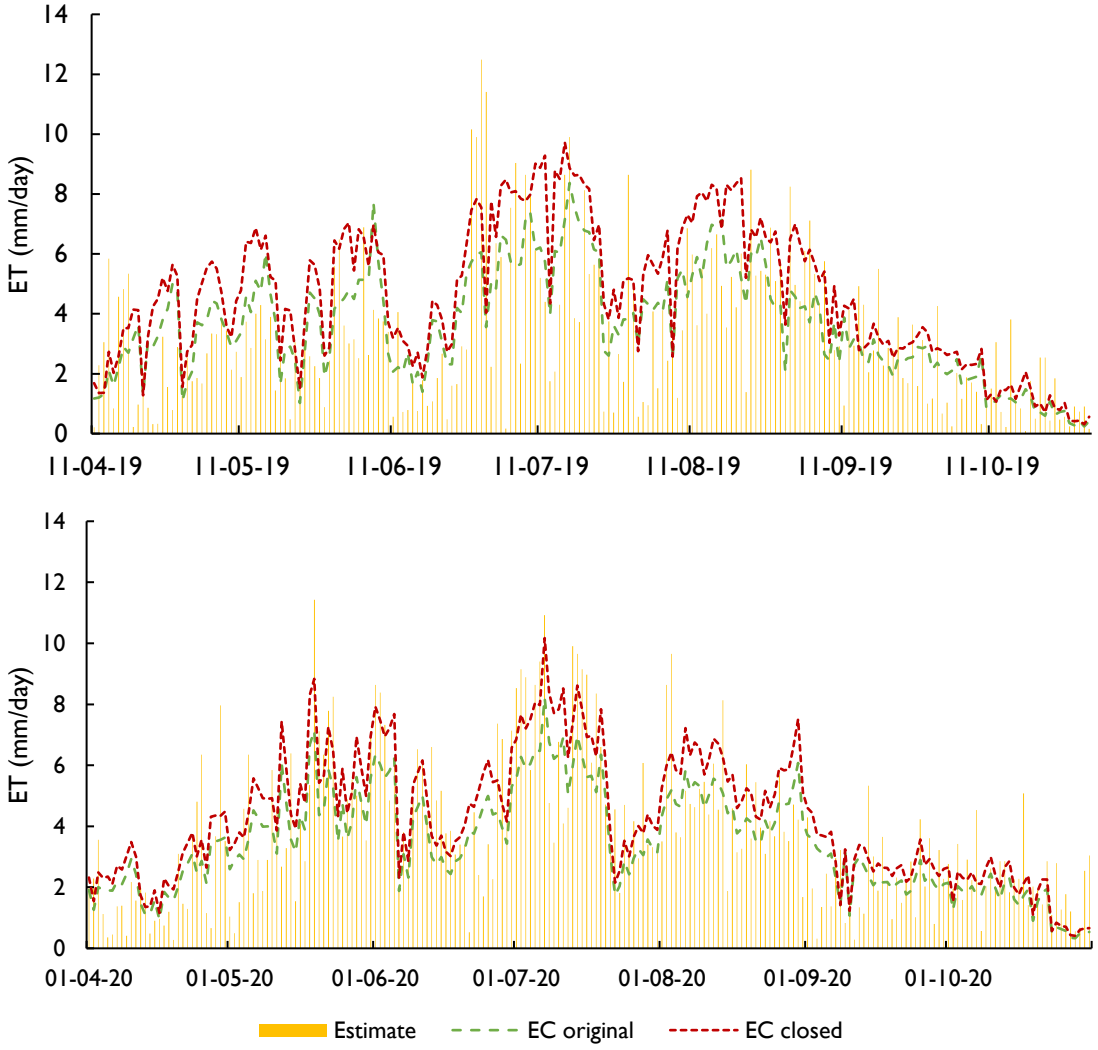

Figure 11: The estimates given by the first attempt at solving the water balance method using only soil moisture data and ETr compared to the EC tower measurement for the Vernal project site in 2019 (top) and 2020 (bottom).

Attempts at improving this method include applying the water balance to each soil layer as represented by the soil moisture sensors (*figure 4*) individually and then summing the individual contributions, applying the method only to the modeled root depth instead of the entire soil profile, and calculating the rate of soil moisture decrease over multiple days. None of these attempts resulted in a significant improvement of the model. For a full description and performance assessment of these improvement attempts see Appendix A.

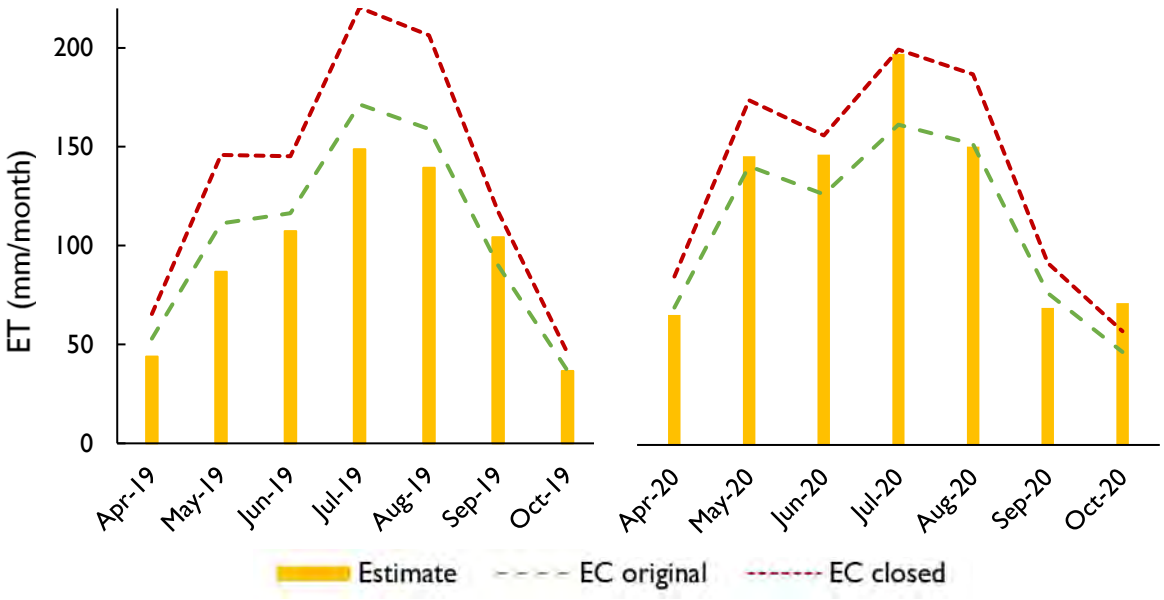

Figure 12: Monthly cumulative values from the water balance approach (vertical bars) and the lower (EC original) and upper (EC closed) limits as measured by the EC flux tower for the Vernal study site in 2019 (left) and 2020 (right).

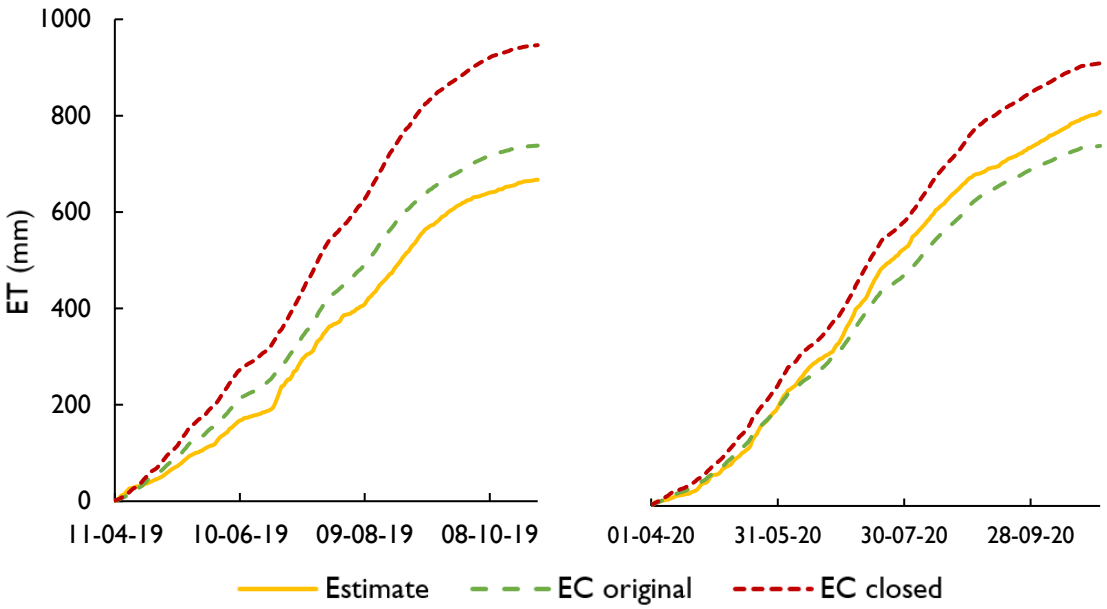

Figure 13: Estimated seasonal cumulative ET values from the water balance approach and the lower (EC original) and upper (EC closed) limits as measured by the EC flux tower for the Vernal study site in 2019 (left) and 2020 (right).

3.2. Preliminary ETa estimation: a hybrid empirical model

Among the top results provided by the Eureqa software (*Figure 14*) a simple trinomial equation using the desired inputs of ETr and $\Delta\theta$ emerged:

Equation 12 $$ETa = aETr + bETr^{+} - c\Delta\theta^{-}$$

Where ETa is the daily ET measured by the EC tower, ETr is the daily reference ET, $\Delta\theta^{-}$ is the daily soil moisture depletion (negative changes in soil moisture), and ETr^{+} is the daily reference ET on days when soil moisture is increasing. *Equation 12* was then split up into a conditional equation based on whether the soil moisture was increasing or decreasing:

Equation 13 $$if\ \Delta\theta < 0 \rightarrow ETr^{+} = 0 \rightarrow ETa = aETr - c\Delta\theta$$

$$if\ \Delta\theta \geq 0 \rightarrow \Delta\theta^{-} = 0 \rightarrow ETa = aETr + bETr$$

Finally, the a, b, and c parameters were combined into a single α value, giving the following conditional equation:

Equation 14 $$if\ \Delta\theta < 0 \rightarrow ETa = \alpha(ETr - \Delta\theta)$$

$$else\ ETa = 2\alpha ETr$$

Where α is an adimensional constant and ETa, ETr and $\Delta\theta$ are in mm/day. Equation 14 is what will be referred to as the Soil Moisture based EvapoTranspiration estimation (SMET) model.

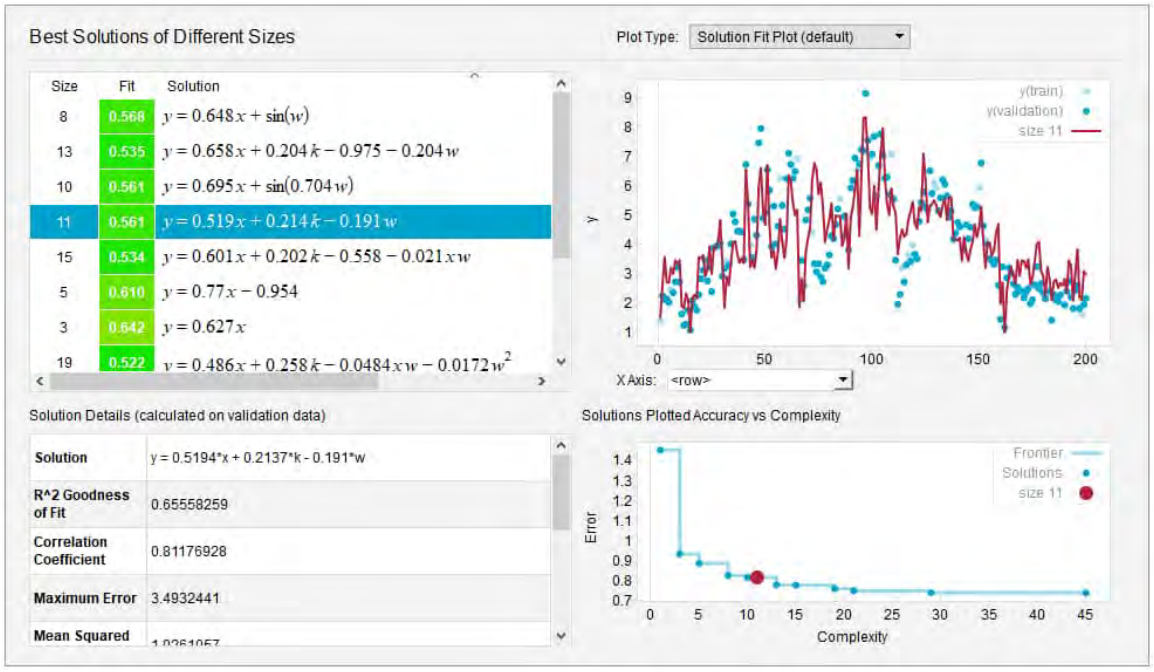

Figure 14. Eureqa solutions tab. The highlighted solution (top right) was selected due to its simplicity. y represents daily ETa as measured by the EC tower, x is daily reference ET, k is daily ETr when soil moisture is increasing, and w is the daily soil moisture depletion.

3.3. Vernal study site: SMET model optimization

The optimization of the α constant was performed by applying the SMET model (*Equation 9*) to the combined 2019 and 2020 datasets collected at the Vernal study using an initial value of $\alpha = 0.30$; this initial value for α was selected as an approximate average of the a, b, and c parameters provided by the Eureqa model (*Equation 12, Figure 14*). The residuals and the RMSE were then calculated and used to fit the equation as described in section 3.1, yielding an optimized value for α of 0.43. The optimized model was then used to calculate the daily ET estimates and the cumulative monthly and cumulative seasonal values for the 2019 and 2020 growing seasons (*Figures 15, 16, and 17*).

The estimated statistics for the SMET model show an increased performance over the water balance method presented in Section 3.1 the r, RMSE, and RRSE were calculated from the daily estimates (*Table 3*): the greater r and lesser RMSE and RRSE values indicate that the SMET model is outperforming the water balance approach presented in section 3.1.

Table 3: Summary statistics for the daily SMET estimates for the 2019 and 2020 growing seasons.

Year	**r**	**RMSE**	**RRSE**
2019	0.76	1.37 mm	0.67 mm
2020	0.81	1.15 mm	0.63 mm

The second verification of the SMET model performance comes from comparing the monthly and seasonal cumulative values from the estimates to the EC tower measurements. Although the model is underestimating cumulative ET in several monthly instances it is more accurate than the water balance approach and, most importantly, it is accurate for the seasonal estimate of both years (*Table 4*).

Table 4: Total seasonal ET as measured by the EC tower and as estimated by the proposed SMET model.

Year	**$ET_{EC\ original}$**	**$ET_{EC\ closed}$**	**ET_{SMET}**
2019	737 mm	945mm	779 mm
2020	738 mm	907 mm	872 mm

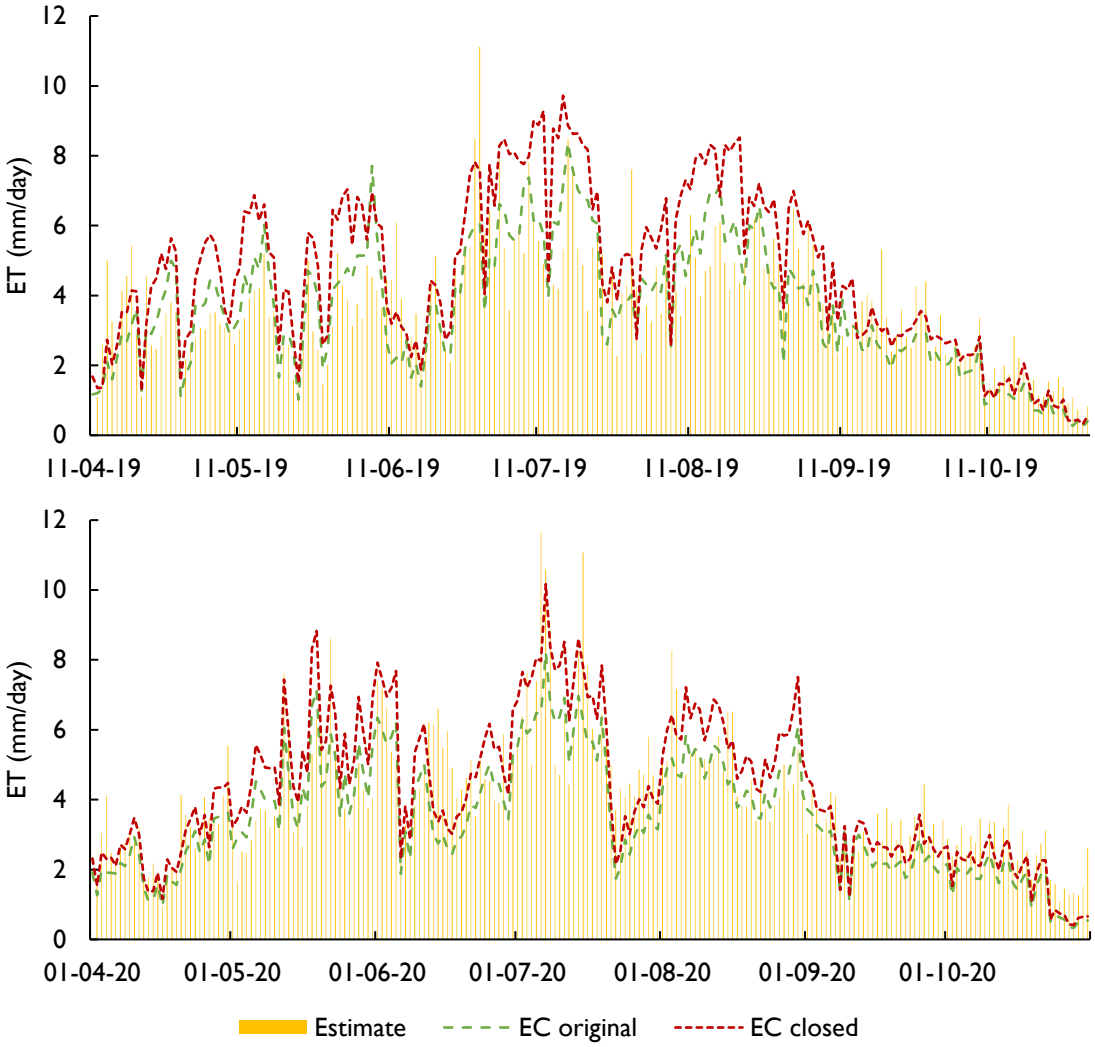

Figure 15: Daily estimates given by the SMET model alongside the EC tower measurements for the Vernal study site in 2019 (top) and (2020).

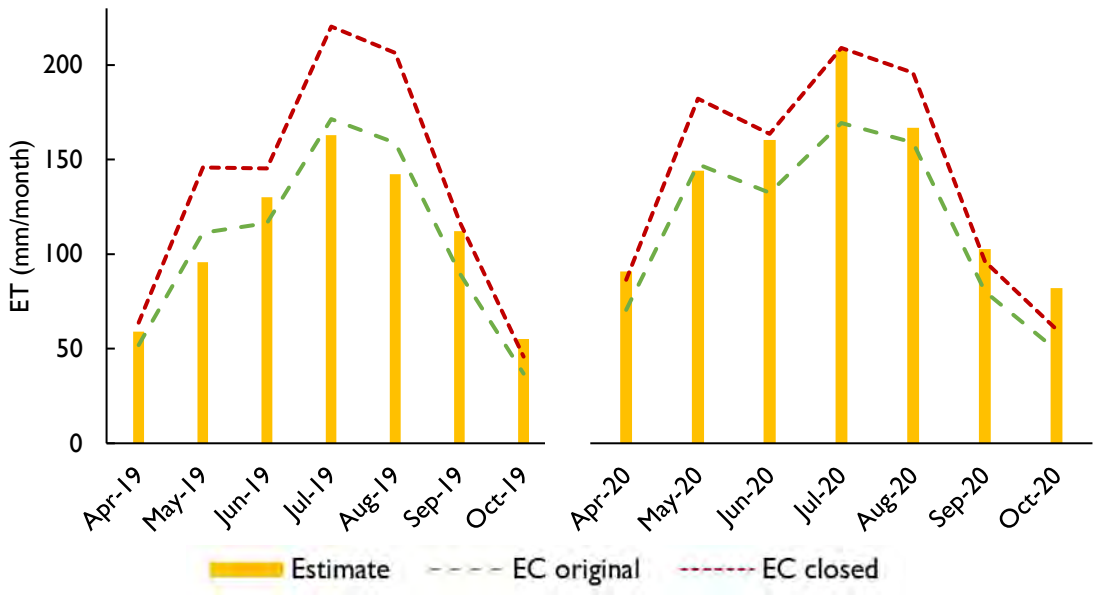

Figure 16: Comparison of the monthly cumulative values from the SMET model and the EC tower measurements for the Vernal study site in 2019 (left) and 2020 (right).

By separating the irrigation from the non-irrigation days, during which soil moisture is increasing or decreasing respectively (*Equation 14*), the SMET model can provide some insight into the irrigation treatment in the absence of such data. For the Vernal site the irrigation there were 24 and 27 days for the 2019 and 2020 years respectively and the ET occurring during those days amounted to approximately 16 and 19% respectively (*Table 5, Figure 17*).

Table 5: Irrigation information inferred from the SMET model for the 2019 and 2020 growing seasons in Vernal.

Year	Total days	Irrigation days		ET during irrigation days	
2019	203	24	12%	116 mm	16%
2020	213	27	13%	138 mm	19%

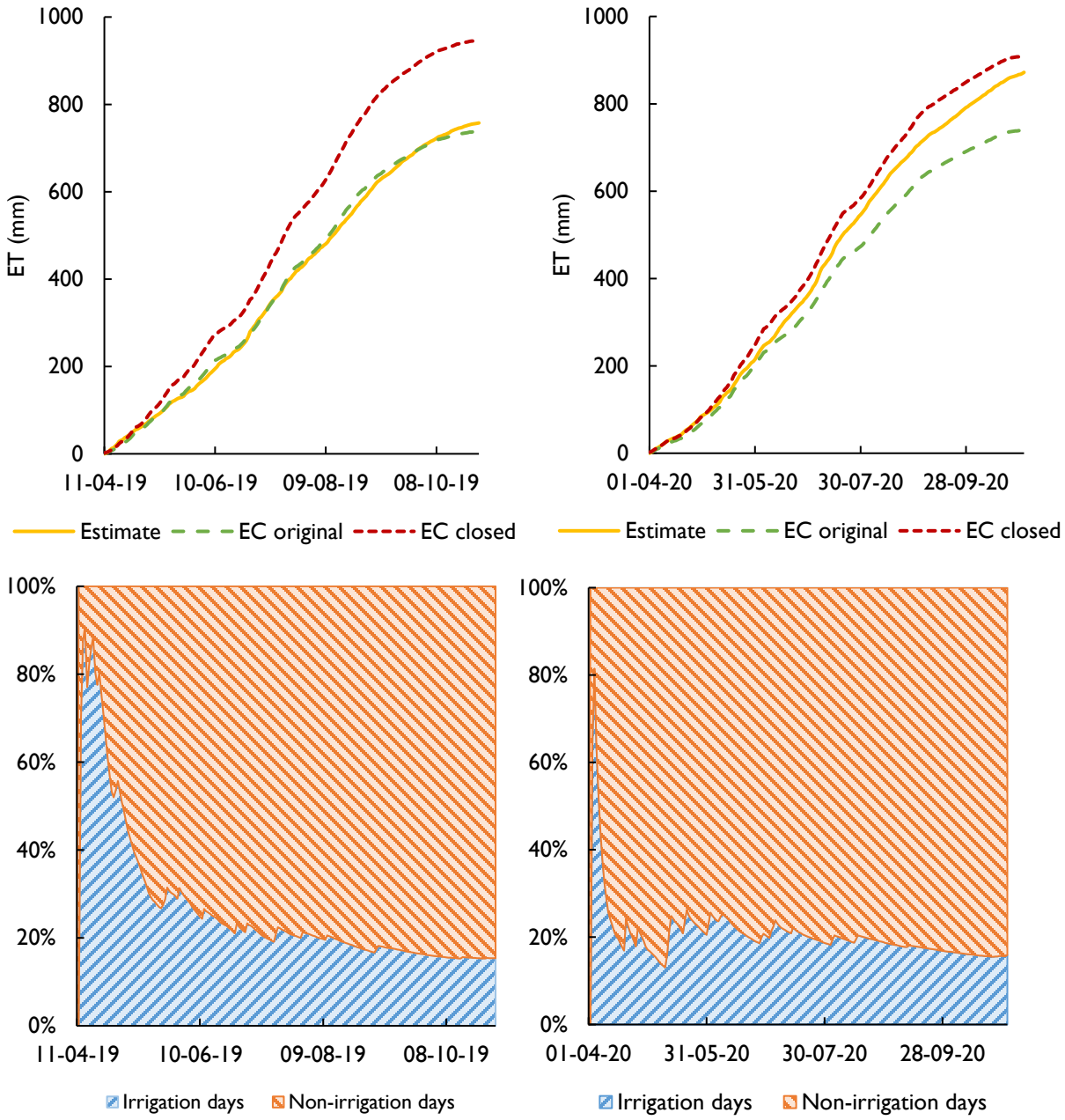

Figure 17: SMET model results for the 2019 and 2020 growing seasons at the Vernal study site. The Seasonal cumulative estimates of both 2019 (top left) and 2020 (top right) are within the EC tower measurements. The total amount of irrigation occurring during irrigation days is 16% for 2019 (bottom left) and 19% for 2020 (bottom right).

3.4. Modena: SMET model verification

The optimized SMET model, with the same α value obtained from the calibration performed with the Vernal data in section 3.3, was applied to the Modena study site in two locations (*Figure 1*) using the soil moisture and ETr data during the 2021 growing season from April 1st to October 22nd, 2021, to calculate cumulative ET yielding a field average value of 1114 mm which is within the range measured by the EC tower of 1032-1191 mm (*Equation 15, Figure 18, Table 6*).

Equation 15

$$ET_{SMET} \in \left[ET_{EC\ original}, ET_{EC\ closed}\right] \rightarrow$$

$$\rightarrow 1114\ mm \in [1032, 1191]\ mm$$

These results show that as long as the fundamental conditions (i.e., deep sensor array, crop canopy completely covers the surface) are not violated, the SMET model can successfully be applied to sites other than the one used for its calibration to obtain reasonable estimates of ET on a seasonal scale.

Table 6: Seasonal ET values for the Modena study site.

$ET_{EC\ original}$	$ET_{EC\ closed}$	$ET_{Field\ estimate}$	$ET_{SMET\ North}$	$ET_{SMET\ East}$
1032 mm	1191 mm	1079 mm	1034 mm	1194 mm

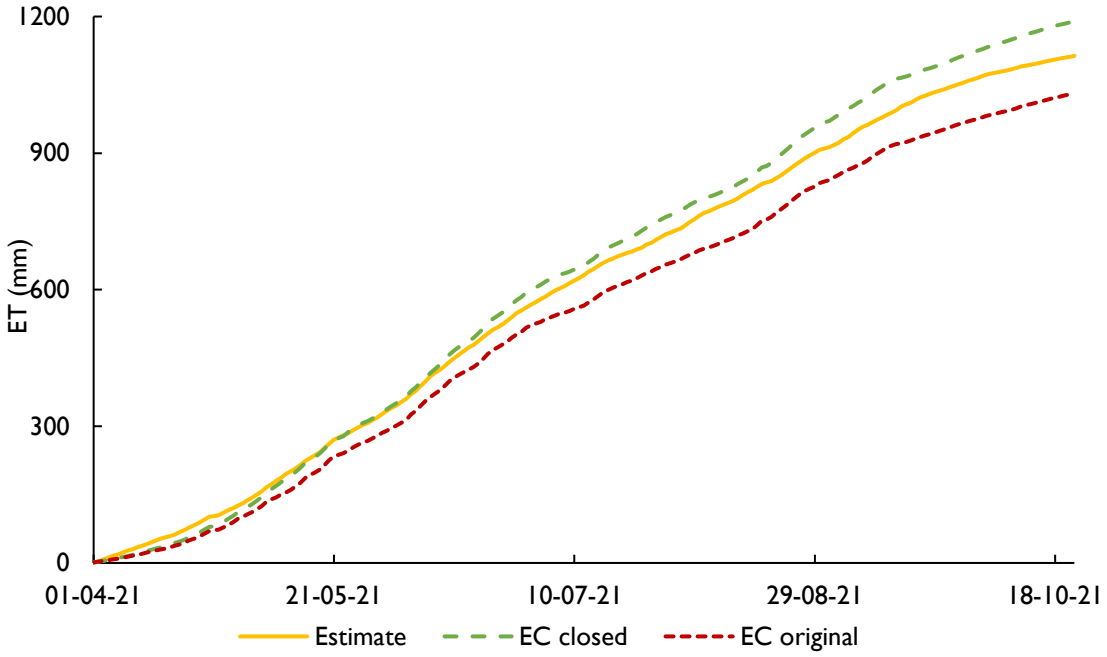

Figure 18: SMET model ET estimate for the 2021 growing season at the Modena study site compared to the EC tower open and closed measurements.

Similarly to what was done in section 3.3 for the Vernal study site, the SMET model can provide some insight on the irrigation treatment applied to the field by separating irrigation and non-irrigation days. The estimated number of irrigation days in for the North and East locations in the field were 61 (30%) and 57 (28%) respectively and the amount of ET that occurred during those days was 27% and 29% respectively (table 7 and figure 19). It is worth noting that these are not the actual number of irrigation days but just an estimate based upon increases in soil moisture, which explains why the North and East location do not match even thought they were irrigated the same amount.

Table 7: SMET model irrigation days estimates for the Modena study site during the 2021 growing season.

Site	Total days	Irrigation days		ET during irrigation days	
North	204	61	30%	362 mm	27%
East	204	57	28%	344 mm	29%

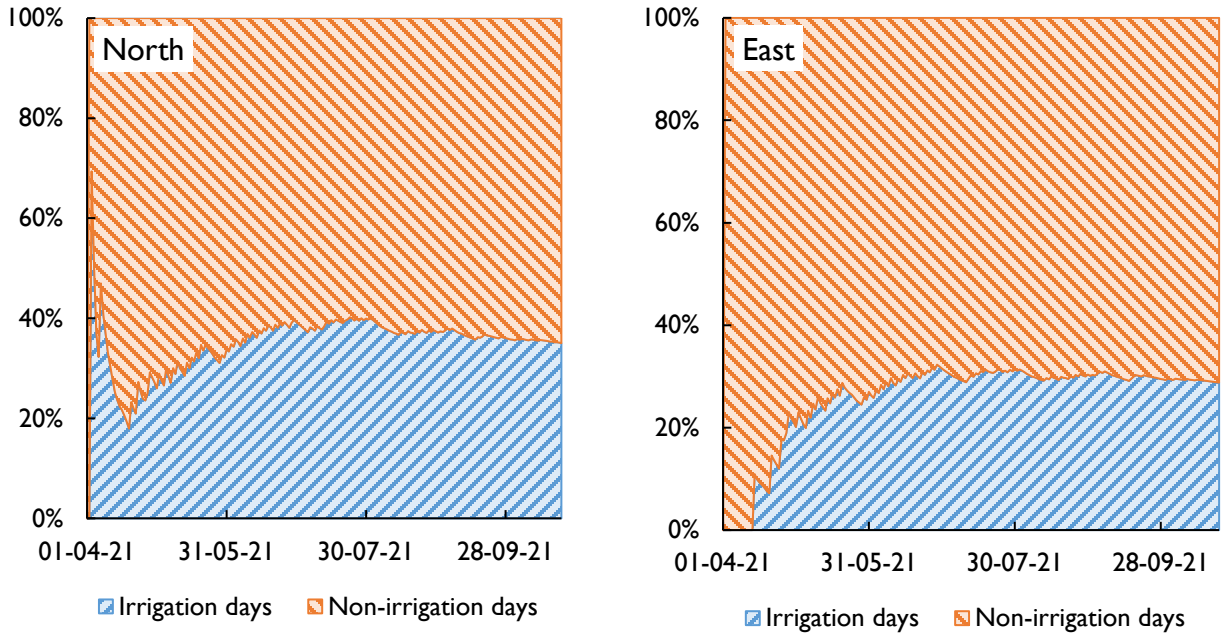

Figure 19: SMET model ET estimate separation during irrigation and non-irrigation days for the 2021 growing season in the North (left) and East (right) locations in the Modena study site

3.5. West Weber: practical application of the SMET model

Since the sensors in the West Weber study sited were installed in an array that allowed to measure the soil moisture under both the onion bed and the furrow, the cumulative ET for each of them was calculated using *Equation 9* with the optimized α presented in section 3.2, from June 27th to August 18th, 2019. The ET values from the bed and the furrow were then averaged as described in section 2.6.2 to obtain a field value that can be used to calculate the total water requirements for both fields. For the flood irrigated field total ET was 316 mm and for the drip irrigated field total ET was 300 mm which is a difference of about 5% (*Figures 19 and 20, Table 8*). While it is expected that the WUE of the drip field is higher than that of the flood irrigated field (Al-Jamal et al. 2001; Halvorson et al. 2008), it is unclear how much of the excess water applied to the flood irrigated field is actually transpired by the plants and how much is lost due to deep percolation and runoff. These results show that ET estimated from the drip irrigated field is about 95% of the ET estimated from the flood irrigated field. Although there is some uncertainty in the absolute values of the ET estimated for the two fields due to a lack of calibration of the α parameter to onions, the ratio of the values should hold true. Additionally, this method allowed to show how the difference in ET for the flood irrigated field and the drip irrigated field is not due to a difference in plant transpiration but rather evaporation from the furrow. As seen in *Table 8* the ET from the bed of the flood irrigated and the drip irrigated fields are the same, but the furrow of the flood irrigated field evaporated 40 mm of water more which is

approximately 17%. This was to be expected as trickle irrigation is designed to satisfy crop water requirements without a large amount of water being evaporated from the soil surface (Keller and Bliesner 1990).

Table 8: West Weber study sites average cumulative ET for the onion bed and the furrow.

	Flood irrigated	Drip irrigated
Onion bed	342 mm	343 mm
Furrow	279 mm	239 mm
Average	316 mm	300 mm

To get an estimate of the volume of water required to irrigate the crop one must simply multiply the depth by the surface area while remembering that $1Ha = 100m \cdot 100m$ and $1m \cdot 1m \cdot 1mm \approx 1l$. Using the field areas from *Table I*:

$$ET_{Flood} = 316\ mm \cdot 3\ Ha = 9.6 \cdot 10^6\ l\ \equiv 9.6 \cdot 10^3\ m^3$$

$$ET_{Drip} = 300\ mm \cdot 7\ Ha = 2.1 \cdot 10^7\ l \equiv 2.1 \cdot 10^4\ m^3$$

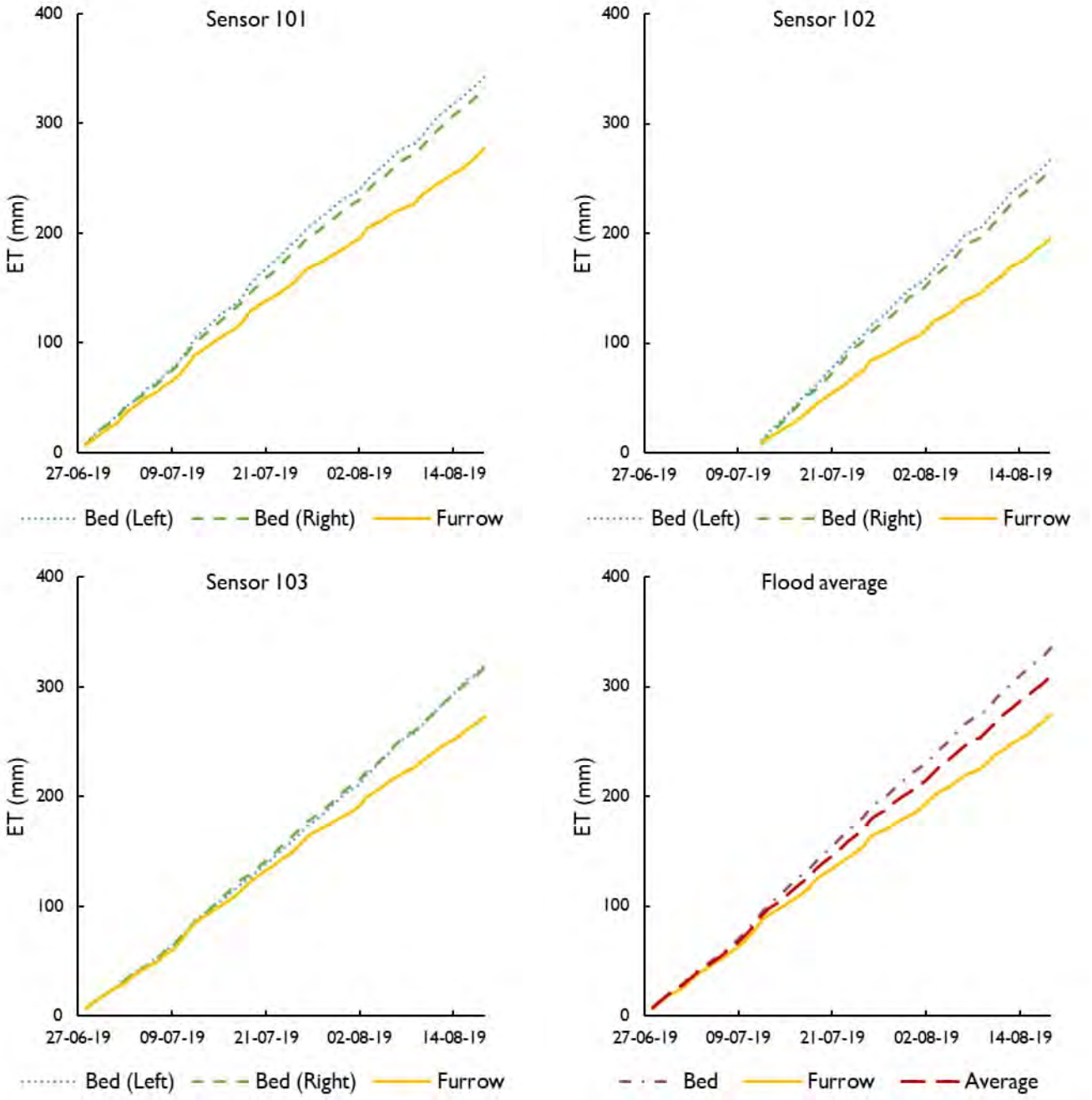

Figure 20: Cumulative ET values estimated with the SMET model for the flood irrigated onion field in West Weber during the 2019 growing season.

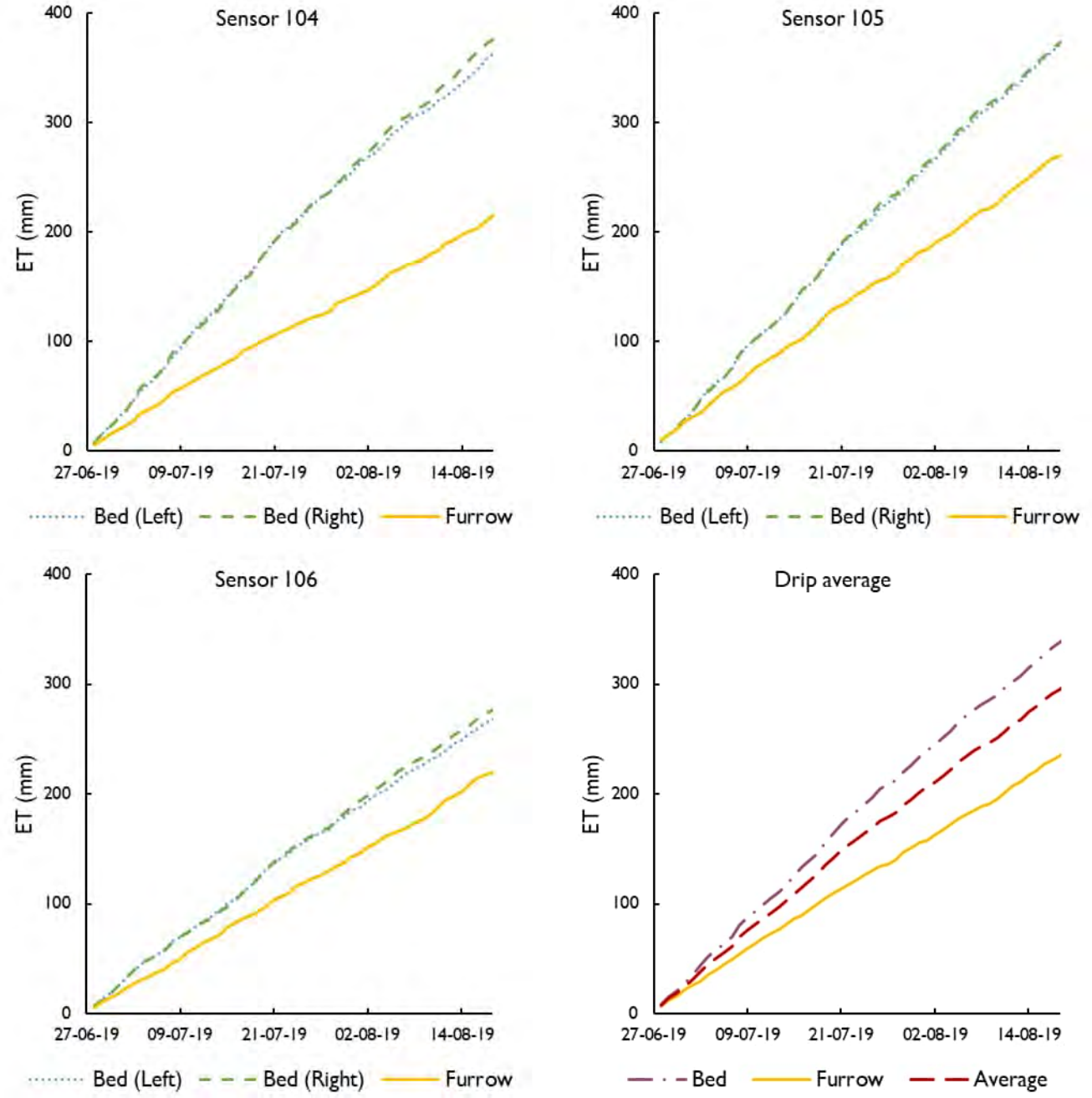

Figure 21: Cumulative ET values estimated with the SMET model for the drip irrigated onion field in West Weber during the 2019 growing season.

3.6. SMET model considerations

Soil moisture sensor depth

The total amount of plant available water is the sum of the available water from all soil horizons occupied by the plant roots (Keller and Bliesner 1990), therefore for this method to work properly it is imperative that the soil moisture data be collected from the entire root zone. Typical root depths can be found in literature (e.g., FAO 56) but actual depth may vary from site to site and should therefore be locally checked (Keller and Bliesner 1990).

Time scale

It is important to note that while the proposed SMET model calculates ET on a daily basis, it does so only as an intermediate step to calculate cumulative values and it is not designed to work on a daily or even weekly time scale. The SMET model is shown to work on seasonal scale in this study, and although further investigation is required it is possible that it will work on a monthly scale. Additionally, it is important to note that since the algorithm calculates daily ET values, the model cannot handle gaps that cannot be filled with reasonable estimates and therefore requires continuous soil moisture and ETr data to function properly.

Potential challenges with drip irrigation

Due to the nature of drip irrigation scheduling being small but frequent, the SMET model might be skewed in favor of using the ETr term more often than the $\Delta\theta$ term because the days when $\Delta\theta>0$ are more frequent than in a sprinkler irrigated field. This limitation can be mitigated by using a deep soil moisture sensor array that will not be overly sensitive to a small and shallow irrigation cycle, but further investigation is recommended.

Potential challenges with flood irrigation

Flood irrigated systems can potentially incur the opposite problem faced by drip irrigated systems, since the irrigation events are designed to saturate the root zone. Excessive deep percolation can introduce errors in the ET estimation process due to large amounts of water moving through the profile, this was observed with a heavy irrigation event that occurred in the Vernal study site on June 26th, 2019, which created a large spike in the results before the outlier detection and correction algorithm was implemented (*Equation 11*). This issue can be mitigated by attempting to limit the saturation of the soil profile to the root zone and by spacing out the irrigation events to ensure that the soil is completely drained and well below field capacity before irrigation occurs. As mentioned in section 2.5, the R code version of the method has an outlier correction algorithm that effectively eliminates any outliers due to this problem.

4. CONCLUSIONS

The main finding of this study is that the proposed SMET model is capable of reliably estimating seasonal ETa with satisfactory accuracy using solely soil moisture and

weather data fulfilling the expectations mentioned in section 2.6 and expressed by *Equation 9* that ETa is a function of both the soil water state (water supply) and the climactic conditions (water demand). This estimate can be obtained from *Equation 14* with a value of α=0.43 and was within the range measured by the EC tower in all study sites. This α value will require further calibration and verification using the same methodology used in this study for other crops and climates. Nonetheless, since it is a multiplicative constant, the results obtained from the model can be used to make relative comparisons by calculating the ratios of ET values for different fields as was done for the West Weber study sites. Additionally, the SMET model works well when large biomass changes occur as demonstrated by the fact that several alfalfa cuts were performed during the growing seasons in Vernal and Modena.

The significance of this finding lies within the simplicity of the data collection and the ease of implementation of the method that allow any land manager to obtain a reasonable estimate of the seasonal water demands with minimal capital investment and labor.

5. FUTURE WORK

Possible future applications include any area where soil moisture sensors can be installed but the heterogeneity of the landscape and the plants make it impractical to use EC flux towers or lysimeters for example in both urban and natural areas. Another example where the SMET model can prove useful is in agricultural research setting where the experimental design splits up the study site into many smaller units with different treatments; in such a setting an EC tower could not pick up the subtle

differences in the treatment units and installing micro lysimeters would prove very laborious and expensive when compared to soil moisture sensor arrays. Additionally, the SMET model could provide useful insight is when used in conjunction with an EC tower in a heterogeneous setting to assess where the total average ET value from the tower can be used to calibrate the model which can then provide a finer resolution of where the water consumption is occurring, similar to how the results from the West Weber study sites gave insight on the difference in ET from the bed and the furrow.

Something that was not investigated in this study but that could prove to be a powerful tool is to use the SMET model to infer root zone soil moisture from ET measurements by inverting *Equations 9, 10, and 11*. This would prove especially interesting in a scenario where the input ET data could be remotely sensed via drones or via satellite (e.g., using the OpenET platform), allowing for root zone soil water content estimates. Note that in order to perform such analysis the irrigation and precipitation days must be known.

CONVERSIONS

$1cm = 10mm = 0.39\ in$

$1m = 100\ cm = 3.28ft$

$1Ha = 10^4\ m^2 = 2.47\ ac$

$1\ m^3 = 10^3 l$

$1l = 10^3\ cm^3 = 0.26\ gal$

ACRONYMS AND SYMBOLS

EC: Eddy covariance

ET: evapotranspiration

ET_a: actual evapotranspiration, *Equation 3*

ET_{closed}: eddy covariance ET after closure

$ET_{original}$: eddy covariance ET before closure

ET_r: reference evapotranspiration

FAO: Food and Agriculture Organization

MAE: mean absolute error

P: precipitation

PM: Penman-Monteith

RMSE: root mean square error

RRSE: relative root square error

RO: runoff

SM: soil moisture

VMC: volumetric water content

WUE: water use efficiency

Δθ: water storage change

APPENDICES

Appendix A. Extended description of previous ET estimation methods

In order to estimate ET six models were developed, the first three (methods A, B, and C) derive an estimate by applying the water balance on a daily scale, the other three (methods D, E, and F) derive an estimate by calculating the slope of the of the soil moisture curve in what will be referred to as the "slope method".

1. Model description for methods A, B, and C

Methods A, B, and C attempt to solve the water balance as described in section 2.6 by assuming that RO, G, and DP are small enough to be neglected.

Assumption 1: $RO = G = DP \approx 0$

This means that the ET rate can be calculated as a function of only P, I, and Δθ.

$$\Delta\theta = P + I - ET$$

These assumptions are made to simplify the ET estimation but cannot be considered to be generally true. In reality G depends on the water table depth. DP and RO largely depend on the irrigation technology, while they are small (or even zero) in a drip irrigated system, this is not the case with a flood irrigation system.

Since precipitation in the project sites during the growing season is infrequent and light it will be considered as negligeable when compared to the irrigation amount and can therefore be incorporated into it:

Assumption 2: $P \ll I \rightarrow P + I \approx I$

This assumption, which can easily be verified a posteriori using local meteorological data, further simplifies the water balance:

$$\Delta\theta = I - ET$$

Finally, since accurate irrigation measurements are not always readily available, the algorithms developed for this project are not designed to produce an estimate of ET during irrigation days. This has the added benefit of mitigating the error due to *assumption 1* since the greatest RO and DP are observed during irrigation.

Assumption 3: $I = 0$

This leaves us with a very simple water balance where ET only depends on θ:

$$\Delta\theta = ET$$

Methods A, B and C use the water balance and *Assumptions 1, 2, and 3* to estimate ET.

1.1. Method A

Method A applies the simplified water balance described above to the entire soil profile at once. The midnight soil moisture value of each day is compared with the midnight soil moisture value of the previous day to determine how much water is consumed.

$$ET_{i-1} = (\theta_{i-1} - \theta_i)z$$

1.2. Method B

Method B applies the simplified water balance described above to each layer of the soil profile individually and then sums the contributions to obtain the total daily value. Essentially, method A is applied to every soil layer using its soil moisture data to obtain the daily ET contribution from that layer.

$$ET_{j,i-1} = (\theta_{j,i-1} - \theta_{j,i}) \cdot (z_j - z_{j-1})$$

$$ET_{Total,i} = \sum_j ET_{j,i}$$

The advantage of this method is that it allows for a more capillary analysis on where the plants are extracting the water from. Additionally, method B allows to neglect negative contributions from any individual soil layer by setting any negative ET value to zero before calculating the total for the entire soil profile, this is done to avoid underestimating ET due to downward water movements when assumption 1 is not true.

1.3. Method C

Method C applies the simplified water balance described above to each soil layer individually just like method B, but additionally accounts for root growth. It does so by automatically assigning a daily ET (ET_j) value of a certain soil layer a value of zero if the modeled root depth (z_R) is not within the depth of said soil layer (z_j).

$$if\ z_R < z_j \rightarrow ET_j = 0$$

If the modeled root depth is within a certain soil layer, the method will only consider the contribution of that layer up to the root depth.

$$if\ z_{R,i} \in [z_j, z_{j+1}] \rightarrow ET_{j,i} = (\theta_{i-1} - \theta_i) \cdot (z_R - z_j)$$

If the root depth is greater than the soil layer depth the daily ET value is estimated as described in method B.

$$if\ z_R > z_j \rightarrow ET_{j,i-1} = (\theta_{j,i-1} - \theta_{j,i}) \cdot (z_j - z_{j-1})$$

As was done for method B, before the total value for the soil profile is calculated, any negative contribution from a single soil layer is set to zero.

$$if\ ET_{j,i} < 0\ \rightarrow\ ET_{j,i} = 0$$

Finally, all the daily ET contributions from the individual soil layers are summed to obtain the total daily value.

$$ET_{Total,i} = \sum_j ET_{j,i}$$

2. Model description for methods D, E, and F

Methods D, E, and F still use the water balance but operate under a new set of assumptions. The first new assumption is that after an irrigation event the soil moisture exceeds the field capacity; this can be verified by looking at the soil moisture content graph if the field capacity is known. Generally, this is the case for flood and often also for sprinkler irrigated systems but not for drip irrigated ones.

Assumption 4: $\theta_i > \theta_{FC}$

The second new assumption is that once field capacity is reached deep percolation and runoff become negligeable, which is coherent with the definition of field capacity.

Assumption 5: if $\theta_i \leq \theta_{FC} \rightarrow RO = DP = 0$

The third and final new assumption is that as long as the soil moisture is decreasing, irrigation and precipitation are negligeable which should be intuitively obvious.

Assumption 6: if $\theta_i \leq \theta_{i-1} \rightarrow I_i = P_i = 0$

Similarly, to methods A, B, and C, these assumptions greatly simplify the water balance resulting in ET being a function of only θ.

$$\Delta\theta = ET$$

The theory behind this approach is that the soil moisture content after an irrigation event often exceeds field capacity ($\theta_i > \theta_{FC}$) and possibly reaches saturation. When this happens, water will drain quickly due to gravity until soil moisture content reaches field capacity ($\theta_i = \theta_{FC}$). At field capacity gravity is no longer removing large amounts of water from the soil and any decrease in soil moisture content can be attributed to plant consumption (ET). The

point in time when $\theta_i = \theta_{FC}$ can often be easily identified visually as the inflection point of the soil moisture content plot (*Figure A*).

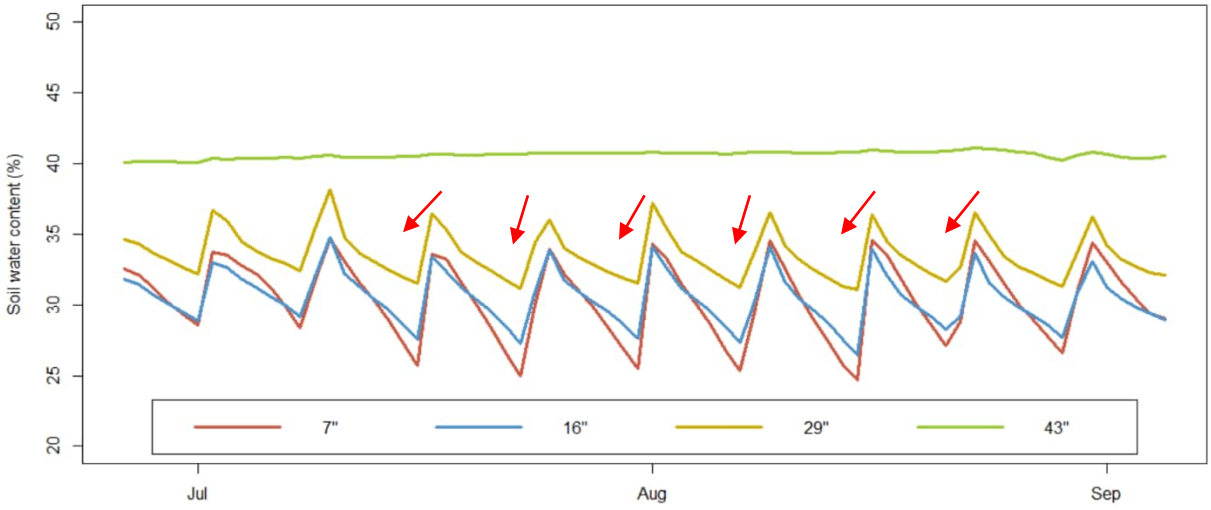

Figure A1: Example of visual assessment of the change in slope when field capacity is reached.

To identify these inflection points mathematically, the first and second derivative of the soil moisture curve need to be calculated.

$$\theta' \equiv \frac{d}{dt}\theta \, , \theta'' \equiv \frac{d}{dt}\theta' \equiv \frac{d^2}{dt^2}\theta$$

The first derivative allows to discern whether the soil moisture content is increasing or decreasing. A decrease in SM can be attributed to either DP or ET (or both). An increase in SM is attributed to an irrigation (or precipitation) event.

$$\theta' < 0 \rightarrow SM\ is\ decreasing: ET\ and/or\ DP$$

$$\theta' > 0 \rightarrow SM\ is\ increasing: P\ and/or\ I$$

The second derivative allows to identify the inflection points in the soil moisture curve and to discern irrigation events from the transition between deep percolation and pure ET:

$$\theta'' < 0 \rightarrow Irrigation\ event$$

$$\theta'' > 0 \rightarrow\ transition\ from\ DP\ to\ ET$$

Now that the part of the SM curve that is not influenced by either irrigation or deep percolation the ET estimation simply becomes the rate of SM decrease which has already been calculated as the first derivative:

$$if\ \theta' < 0\ \wedge\ \theta'' > 0 \rightarrow ET = \theta'$$

Since the daily soil moisture data is discrete rather than continuous it is impossible to calculate the actual derivatives so instead a linear regression with the values of the previous and subsequent days is calculated. The slope of this regression can then be used as an approximation of the actual derivatives.

$$y = lm(\theta_{i-1}, \theta_i, \theta_{i+1}) \rightarrow \theta' \cong slope(y)$$

2.1. Method D

Method D applies the slope method to the entire soil profile at once. In order to do so the soil moisture data from the four depths were aggregated into one total soil moisture curve by calculating the weighted average:

$$\theta_{total,i} = \sum_j \theta_j \cdot z_j$$

2.2. Method E

Method E applies the slope method to each of the soil layers individually and then sums them up to obtain the total value, similarly to method B.

2.3. Method F

Method F applies the slope method to the each of the soil layers individually just like method E but accounts for root growth the same way method C does.

Table A1: Overview of the six water balance methods.

Alias	Method	Description
A	Soil moisture depletion on the entire soil profile.	Daily ET is calculated as the soil moisture depletion between two midnight values for the entire soil profile.
B	Soil moisture depletion on a soil layer basis.	Daily ET is calculated as the soil moisture depletion between two midnight values for each soil layer. Layer values are summed to get the daily ET value for entire profile.
C	Soil moisture depletion on soil layer basis accounting for root growth.	Same as method B but calculations account for root growth.
D	Soil moisture slope on the entire soil profile.	Daily ET is calculated from the 1st and 2nd derivatives of the change in soil moisture for the entire soil profile.
E	Soil moisture slope on a soil layer basis.	Daily ET is calculated from the 1st and 2nd derivatives of the change in soil moisture for each soil layer. Layer values are summed to get the daily ET value for the entire profile.
F	Soil moisture slope on a soil layer basis accounting for root growth.	Same as method E but calculations account for root growth.

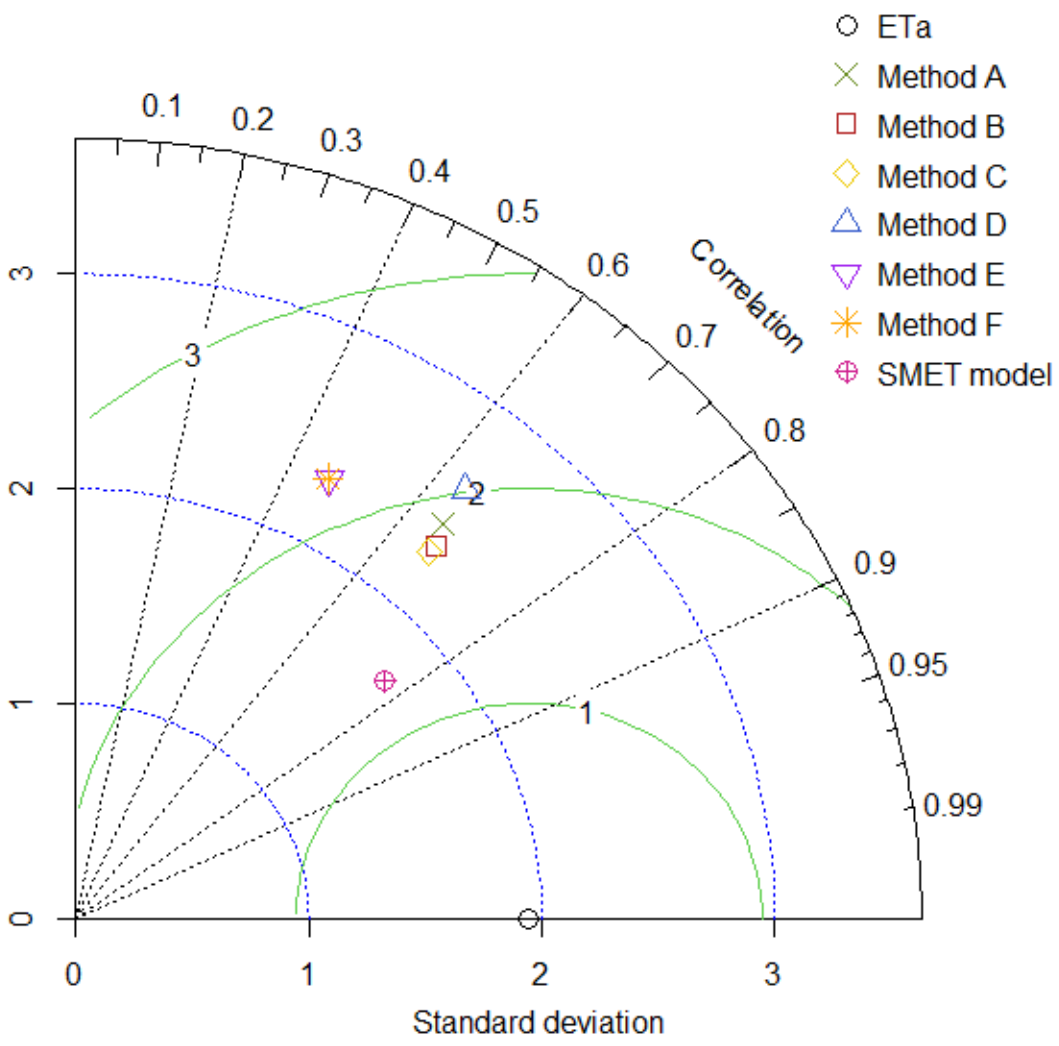

Figure A2: Taylor diagram comparing the performance of the developed ET estimation methods. The blue circles centered in the origin represent the standard deviation of the dataset, the green circles centered in ETa represent the mean absolute error, and the angular distance from the vertical axis represent the correlation with ETa. The SMET model outperforms the other methods by having a closer standard deviation, a smaller mean absolute error, and a higher correlation, when compared to ETa.

Appendix B. Soil moisture profiles

The soil moisture profile plots were generated by plotting the volumetric water content reading (%) against the sensor depth (cm) for the Vernal and Modena study sites. These plots can be used to further one's understanding of how water moves through the soil and how much water is retained by the soil layers with different textures.

Figure B1 and B2 are an example of the soil moisture profile plots around an irrigation event at the Vernal and the Modena study sites respectively. For the animated version consult the electronic version of this document or the following GitHub repository: https://github.com/OliverHargreaves/Soil_Moisture_Profile_Plots.

The soil moisture profile for the Vernal study site (*Figure B1*) shows how the top ~100 cm experience great changes in VWC during and after an irrigation event, with the most dramatic change being in the topmost layers going from ~20% to ~40%. Conversely, at deeper depths (~>100 cm) the VWC remains fairly constant at ~40%, this is presumably because of capillary rise from the water table.

The soil moisture profile for the East location of the Modena study site (*Figure B2*) shows how the water moves downward after an irrigation event. Due to frequent irrigation, the topmost soil layers (~50 cm) at this study site never drain completely and therefore the VWC changes are far less dramatic than at the Vernal study site. The VWC in deeper layers also does not change much due to irrigation and is fairly constant at ~ 10%, this is presumably due to the low water holding capacity of these rocky layers.

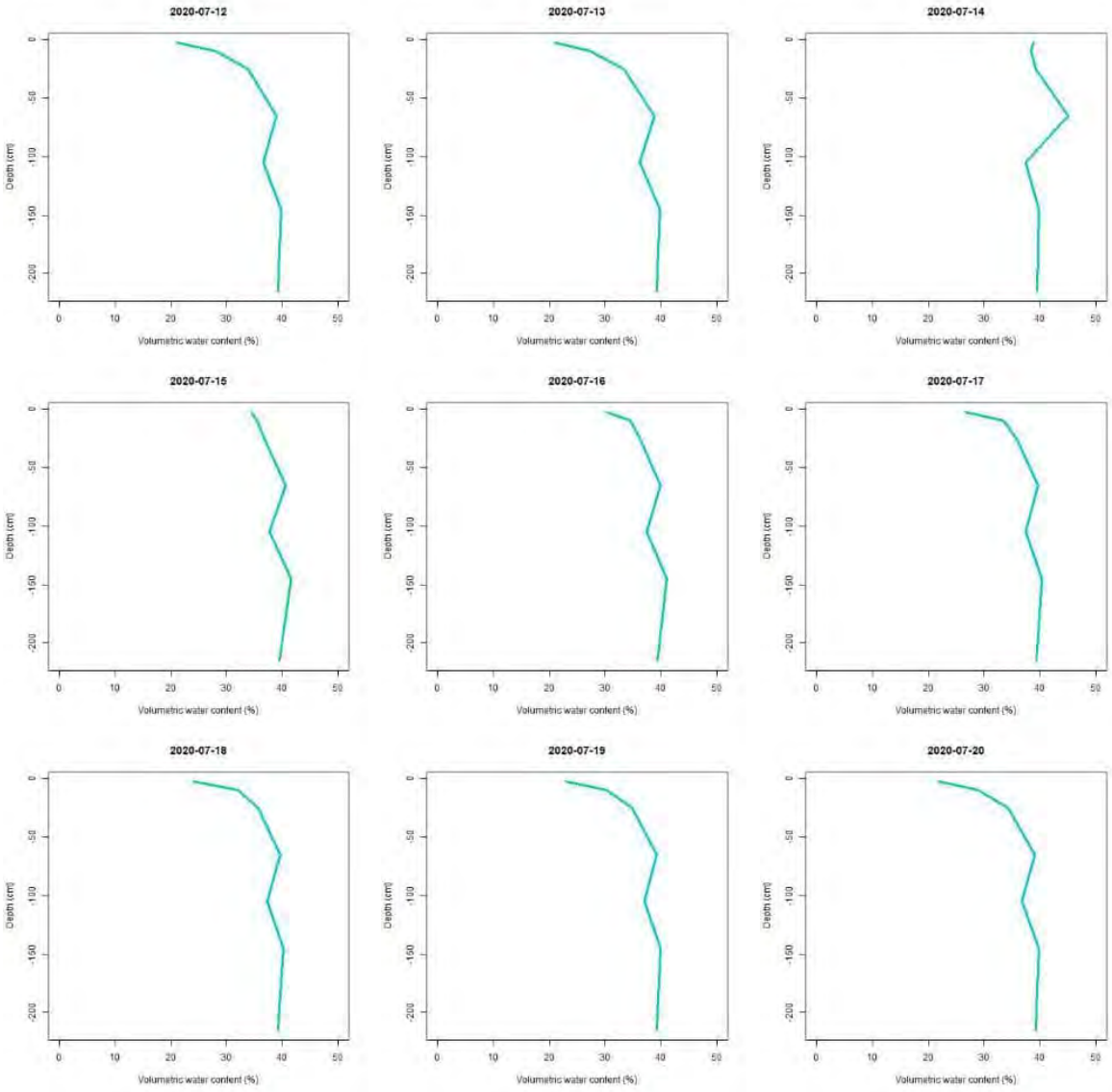

Figure B1: Daily soil moisture profiles from the 12th to the 20th of July 2020 at the Vernal study site. The x-axis represents volumetric water content (%) and the y-axis represents the depth (cm) at which the measurement was taken.

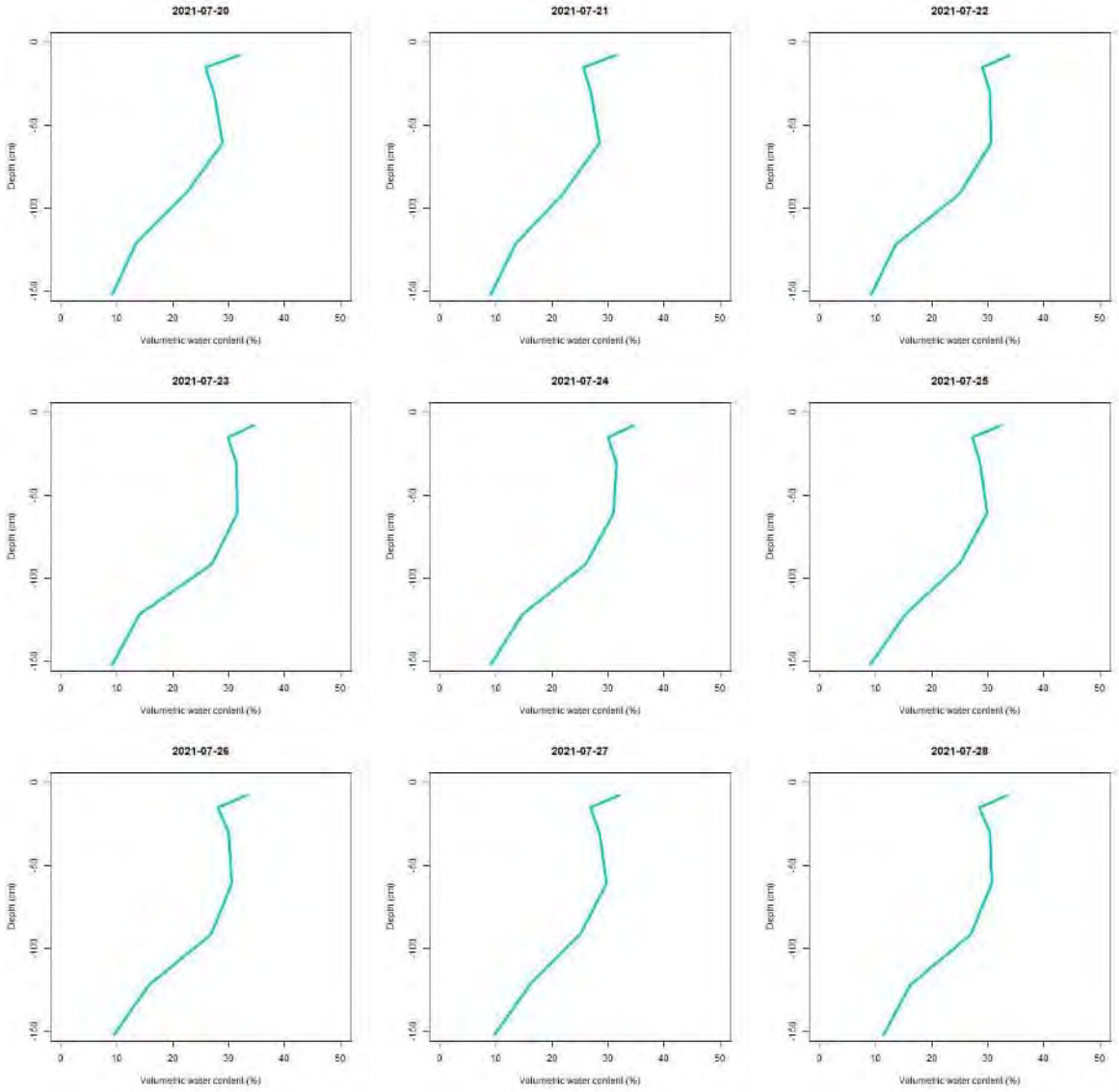

Figure B2: Daily soil moisture profile plots from the 20th to the 28th of July 2021 at the East location of the Modena study site. The x-axis represents volumetric water content (%) and the y-axis represents the depth (cm) at which the measurement was taken.

SOFTWARE

ArcGIS pro v 3.0.0 ESRI inc., Redlands, CA, USA, 2022 https://pro.arcgis.com/en/pro-app/latest/get-started/download-arcgis-pro.htm

ArcMap v10.8.1 ESRI inc., Redlands, CA, USA, 2019 https://desktop.arcgis.com/en/arcmap/latest/get-started/introduction/a-quick-tour-of-arcmap.htm

Eureqa v 1.24.0 Nutonian inc., Boston, MA, USA

Excel v 2210 Microsoft corporation, Redmond, WA, USA, 2022 https://www.microsoft.com/en-us/microsoft-365/excel

R studio v 22.07.02-576 Posit PBC, Boston, MA, USA, 2022 https://posit.co/download/rstudio-desktop/

RefET v 4.1 University of Idaho, Kimberly, ID, USA, 2016 https://www.uidaho.edu/cals/kimberly-research-and-extension-center/research/water-resources/ref-et-software

BIBLIOGRAPHY

Aboutalebi M, Allen N, Torres-Rua AF, et al (2019) Estimation of soil moisture at different soil levels using machine learning techniques and unmanned aerial vehicle (UAV) multispectral imagery. SPIE-Intl Soc Optical Eng, p 26

Acclima Digital TDR Soil Moisture Sensors. https://acclima.com/digital-tdr-soil-moisture-sensors/. Accessed 3 Aug 2022

Acclima (2022) True TDR-315H

Akuraju VR, Ryu D, George B (2021) Estimation of root-zone soil moisture using crop water stress index (CWSI) in agricultural fields. GIsci Remote Sens 58:340–353. https://doi.org/10.1080/15481603.2021.1877009

Al-Jamal MS, Ball S, Sammis TW (2001) Comparison of sprinkler, trickle and furrow irrigation efficiencies for onion production. Agric Water Manag 46:253–266. https://doi.org/10.1016/S0378-3774(00)00089-5

Allen, R. G., Pereira LS, Raes, D., Smith, M. (1998) Crop evapotranspiration guidelines for computing crop water requirements. Rome

Allen RG (1999) Ref-ET: reference evapotranspiration calculation software for FAO and ASCE Standardized Equations

Alonso E. Rhenals, Rafael L. Bras (1981) The Irrigation Scheduling Problem and Evapotranspiration Uncertainty. Water Resour Res 17:1328–1338

Bastiaanssen WGM, Allen RG, Droogers P, et al (2007) Twenty-five years modeling irrigated and drained soils: State of the art. Agric Water Manag 92:111–125

Bureau of Reclamation WaterSMART Water and Energy Efficiency Grants | Bureau of Reclamation. https://www.usbr.gov/watersmart/weeg/index.html. Accessed 23 Jun 2022

Caird MA, Richards JH, Donovan LA (2007) Nighttime stomatal conductance and transpiration in C3 and C4 plants. Plant Physiol 143:4–10

Diarra A, Jarlan L, Er-Raki S, et al (2017) Performance of the two-source energy budget (TSEB) model for the monitoring of evapotranspiration over irrigated annual crops in North Africa. Agric Water Manag 193:71–88. https://doi.org/10.1016/j.agwat.2017.08.007

Drechsler K, Fulton A, Kisekka I (2022a) Crop coefficients and water use of young almond orchards. Irrig Sci 40:379–395. https://doi.org/10.1007/s00271-022-00786-y

Drechsler K, Fulton A, Kisekka I (2022b) Crop coefficients and water use of young almond orchards. Irrig Sci 40:379–395. https://doi.org/10.1007/s00271-022-00786-y

Dubčáková R (2011) Eureqa: Software review. Genet Program Evolvable Mach 12:173–178

Dursun M, Ozden S (2011) A wireless application of drip irrigation automation supported by soil moisture sensors. Scientific Research and Essays 6:1573–1582

FAO Water Management | Land & Water | Food and Agriculture Organization of the United Nations | Land & Water | Food and Agriculture Organization of the United Nations. https://www.fao.org/land-water/water/water-management/en/. Accessed 23 May 2022

Fereres E, Soriano MA (2007) Deficit irrigation for reducing agricultural water use. J Exp Bot 58:147–159. https://doi.org/10.1093/jxb/erl165

Foken T, Foken1 T (2008) The Energy Balance Closure Problem: An Overview

Franssen HJH, Stöckli R, Lehner I, et al (2010) Energy balance closure of eddy-covariance data: A multisite analysis for European FLUXNET stations. Agric For Meteorol 150:1553–1567. https://doi.org/10.1016/j.agrformet.2010.08.005

Gebler S, Hendricks Franssen HJ, Pütz T, et al (2015) Actual evapotranspiration and precipitation measured by lysimeters: A comparison with eddy covariance and tipping bucket. Hydrol Earth Syst Sci 19:2145–2161. https://doi.org/10.5194/hess-19-2145-2015

Gillies RR, Ramsey RD (2009) Climate of Utah. Rangeland Resources of Utah 39–45

Halvorson AD, Bartolo ME, Reule CA, Berrada A (2008) Nitrogen effects on onion yield under drip and furrow irrigation. Agron J 100:1062–1069. https://doi.org/10.2134/agronj2007.0377

Hargreaves GH, Asce F, Allen RG (2003) History and Evaluation of Hargreaves Evapotranspiration Equation. Journal of irrigation and drainage engineering 129:53–63. https://doi.org/10.1061/ASCE0733-943720031 29:153

Hargreaves GL, Asce AM, Hargreaves GH, et al (1985) Irrigation water requirements for Senegal river basin. Journal of Irrigation and Drainage Engineering 111:265–275

Keller J, Bliesner RD (1990) Sprinkle and trickle irrigation

Kimberly Research and Extension Center Ref-ET Software. https://www.uidaho.edu/cals/kimberly-research-and-extension-center/research/water-resources/ref-et-software. Accessed 1 Aug 2022

Kisekka I, Peddinti SR, Kustas WP, et al (2022) Spatial–temporal modeling of root zone soil moisture dynamics in a vineyard using machine learning and remote sensing. Irrig Sci. https://doi.org/10.1007/s00271-022-00775-1

López-Urrea R, Martín de Santa Olalla F, Fabeiro C, Moratalla A (2006) Testing evapotranspiration equations using lysimeter observations in a semiarid climate. Agric Water Manag 85:15–26. https://doi.org/10.1016/j.agwat.2006.03.014

Malek E, McCurdy G, Giles B (1999) Dew contribution to the annual water balances in semi-arid desert valleys. J Arid Environ 42:71–80. https://doi.org/10.1006/jare.1999.0506

Markwitz C, Siebicke L (2019) Low-cost eddy covariance: A case study of evapotranspiration over agroforestry in Germany. Atmos Meas Tech 12:4677–4696. https://doi.org/10.5194/amt-12-4677-2019

Maughan T, Allen LN, Drost D (2015) Soil Moisture Measurement and Sensors for Irrigation Management Soil Water. Extension Utah State University 1:124–130

Melton FS, Huntington J, Grimm R, et al (2021) OpenET: Filling a Critical Data Gap in Water Management for the Western United States. J Am Water Resour Assoc 1–24. https://doi.org/10.1111/1752-1688.12956

Michon Scott, Rebecca Lindsey (2022) Large declines in snowpack across the U.S. West | NOAA Climate.gov. https://www.climate.gov/news-features/understanding-climate/large-declines-snowpack-across-us-west. Accessed 12 Sep 2022

Microsoft Define and solve a problem by using Solver. https://support.microsoft.com/en-us/office/define-and-solve-a-problem-by-using-solver-5d1a388f-079d-43ac-a7eb-f63e45925040. Accessed 16 Aug 2022

Migliaccio KW, Schaffer B, Crane JH, Davies FS (2010) Plant response to evapotranspiration and soil water sensor irrigation scheduling methods for papaya production in south Florida. Agric Water Manag 97:1452–1460. https://doi.org/10.1016/j.agwat.2010.04.012

Murray RC, Reeves EB (1977) Estimated Use of Water in the United States in 1975.

PRISM Climate Group at Oregon State University 30-year normals. https://prism.oregonstate.edu/normals/. Accessed 31 Jul 2022

Ruiz-Peñalver L, Vera-Repullo JA, Jiménez-Buendía M, et al (2015) Development of an innovative low cost weighing lysimeter for potted plants: Application in lysimetric stations. Agric Water Manag 151:103–113. https://doi.org/10.1016/j.agwat.2014.09.020

Schmidt M, Lipson H (2009) Distilling free-form natural laws from experimental data. Science (1979) 324:81–85. https://doi.org/10.1126/science.1165893

Scott CA, Wim ;, Bastiaanssen GM, Ahmad M-U-D (2003) Mapping Root Zone Soil Moisture Using Remotely Sensed Optical Imagery. Journal of irrigation and drainage engineering 129:326–335. https://doi.org/10.1061/ASCE0733-94372003129:5326

Šimůnek J, Genuchten MTh, Šejna M (2008) Development and Applications of the HYDRUS and STANMOD Software Packages and Related Codes. Vadose Zone Journal 7:587–600. https://doi.org/10.2136/vzj2007.0077

Song L, Liu S, Kustas WP, et al (2018) Monitoring and validating spatially and temporally continuous daily evaporation and transpiration at river basin scale. Remote Sens Environ 219:72–88. https://doi.org/10.1016/j.rse.2018.10.002

Trajkovic S, Kolakovic S (2009) Evaluation of reference evapotranspiration equations under humid conditions. Water Resources Management 23:3057–3067. https://doi.org/10.1007/s11269-009-9423-4

Trenberth KE (2011) Changes in precipitation with climate change. Clim Res 47:123–138. https://doi.org/10.3354/cr00953

United Nations Population | United Nations. https://www.un.org/en/global-issues/population. Accessed 23 May 2022

Utah Division of Water Resources Agricultural Water Optimization – Utah Division of Water Resources. https://water.utah.gov/agwateroptimization/. Accessed 23 Jun 2022

Utah State University Utah Climate Center. https://climate.usu.edu/mchd/index.php. Accessed 1 Aug 2022

Victor Hugo de Morais Danelichen, Osvaldo Alves Pereira, Marcelo Sacardi Biudes, José de Souza Nogueira (2021) View of Assessment of spectral indexes for estimating soil water content in the Brazilian Pantanal | Ciência e Natura. In: Geosciences (Basel). https://periodicos.ufsm.br/cienciaenatura/article/view/42724/html. Accessed 23 Jun 2022

Walker WR, Skogerboe G v. (1987) Surface irrigation theory and practice

Wan Z, Zhang K, Xue X, et al (2015) Water balance-based actual evapotranspiration reconstruction from ground and satellite observations over the conterminous United States. Water Resour Res 51:6485–6499. https://doi.org/10.1002/2015WR017311

Wei G, Zhang X, Ye M, et al (2019) Bayesian performance evaluation of evapotranspiration models based on eddy covariance systems in an arid region. Hydrol Earth Syst Sci 23:2877–2895. https://doi.org/10.5194/hess-23-2877-2019

Wharton S (2017) Meteorological Observations Available for the State of Utah

Xu J, Wang J, Wei Q, Wang Y (2016) Symbolic Regression Equations for Calculating Daily Reference Evapotranspiration with the Same Input to Hargreaves-Samani in Arid China. Water Resources Management 30:2055–2073. https://doi.org/10.1007/s11269-016-1269-y

Zotarelli L, Dukes MD, Scholberg JMS, et al (2011) Irrigation Scheduling for Green Bell Peppers Using Capacitance Soil Moisture Sensors. Journal of Irrigation and Drainage Engineering 137:73–81. https://doi.org/10.1061/(asce)ir.1943-4774.0000281